4854 *Chem. Mater.* **2010,** *22,* 4854–4866
DOI:10.1021/cm101443x

CHEMISTRY OF MATERIALS
Article

Solution Reactions of a Bis(pyrrolylaldiminate)copper(II) Complex with Peralkyl Zinc, Aluminum, and Boron Reagents: Investigation of the Pathways Responsible for Copper Metal Deposition

Balamurugan Vidjayacoumar,[†] David J. H. Emslie,*[,†] James M. Blackwell,*[,‡] Scott B. Clendenning,[‡] and James F. Britten[†]

[†]*Department of Chemistry, McMaster University, 1280 Main Street West, Hamilton, Ontario L8S 4M1, Canada, and* [‡]*Intel Corporation, RA3-252, 2501 Northwest 229th Avenue, Hillsboro, Oregon 97124*

Received May 22, 2010. Revised Manuscript Received July 13, 2010

The solution reactions of bis(*N*-isopropylpyrrolylaldiminate)copper(II) (CuL_2) with $AlMe_3$, BEt_3, and $ZnEt_2$ have been studied. In all cases, reduction occurs in two stages via a stable copper(I) pyrrolylaldiminate complex (Cu_2L_2), with each stage initiated by copper alkyl complex formation. Reduction from "LCuR" (R = Me or Et) occurs with release of R_2 or L−R, consistent with bimolecular C−C or C−N bond-forming reductive elimination. At room temperature or below, copper deposition from "CuMe" occurs exclusively via reductive elimination of ethane, whereas decomposition of "CuEt" yields ethylene, ethane, and hydrogen, indicative of both β-hydride elimination and reductive elimination. The reaction byproducts [Cu_2L_2], [$LAlMe_2$], [L_2AlMe], [AlL_3], [$LBEt_2$], [LZnEt], [ZnL_2], L−Me, and L−Et were synthesized independently and isolated as pure compounds. All compounds are thermally stable, with the exception of LZnEt, which undergoes ligand redistribution to form ZnL_2 and $ZnEt_2$ in solution and as a solid at elevated temperatures. With the exception of [LZnEt] and [Cu_2L_2], these complexes are also volatile; monoligated [$LAlMe_2$] and [$LBEt_2$] are particularly volatile, and therefore more desirable as byproducts in ALD or pulsed-CVD.

Introduction

Atomic layer deposition (ALD) is a process of increasing industrial importance by which ultrathin highly conformal films of uniform thickness may be deposited in a self-limiting fashion. In a typical process, this is achieved by performing multiple cycles of the following steps: (1) exposure of a substrate to vapors of a metal precursor, resulting in adsorption of a monolayer, (2) removal of any excess precursor with an inert gas purge, (3) exposure of the surface to an excess of a reactive coreagent (e.g., H_2, H_2O or NH_3) selected to effect deposition of a desired material (e.g., a metal, metal oxide, or metal nitride) upon reaction with the adsorbed metal precursor, and (4) removal of any excess coreagent and volatile reaction byproducts with an inert gas purge. So long as sufficient vapor doses of the metal precursor and coreagent are delivered to ensure maximum surface coverage and complete reaction, film thickness will depend only on the number of precursor/purge/coreagent/purge cycles; this is termed self-limiting behavior.[1] However, if self-limiting behavior cannot be achieved (even in cases where a primary ALD pathway is accompanied by a minor parasitic CVD process), the overall process is termed pulsed-CVD. Copper, which is the focus of this work, has now replaced aluminum as the primary interconnect metal for most microelectronics applications, and as device dimensions decrease, the conformality and uniformity of thin film deposition becomes increasingly important.[2] The development of new and improved copper metal ALD methods is therefore of great importance.

A preceding companion article[3] described studies of copper metal deposition from solution and under ALD/pulsed-CVD conditions, with a focus on the reactions of $AlMe_3$, BEt_3, and $ZnEt_2$ with the copper(II) complexes [CuL_2] [L = acetylacetonate (acac; **1**), hexafluoroacetylacetonate (hfac; **2**), *N*-isopropyl-β-ketiminate (acnac; **3**), *N*,*N*-dimethyl-β-diketiminate (nacnac; **4**), 2-pyrrolylaldehyde (PyrAld; **5**), *N*-isopropyl-2-pyrrolylaldiminate (PyrIm^{iPr}; **6a**),

*Corresponding author. (1) Fax: (905)-522-2509. Tel: (905)-525-9140, x23307. E-mail: emslied@mcmaster.ca (D.J.H.E.); (2) E-mail: james.m.blackwell@intel.com (J.M.B.).

(1) Kim, H. *J. Vac. Sci. Technol., B* **2003**, *21*, 2231. Leskelä, M.; Ritala, M. *Angew. Chem., Int. Ed.* **2003**, *42*, 5548.Leskelä, M.; Niinistö, L.; Pakkanen, T.; Mason, N. J.; Tischler, M. A.; Bedair, S. M.; Yao, T. In *Atomic Layer Epitaxy*; Suntola, T., Simpson, M., Eds.; Blackie: Glasgow, 1990.Ritala, M.; Leskelä, M. Atomic Layer Deposition. In *Handbook of Thin Film Materials*; Nalwa, H. S., Ed.; Academic Press: San Diego, 2001; Vol. *1* − Deposition and Processing of Thin Films, p 103. Niinistö, L.; Päiväsaari, J.; Niinistö, J.; Putkonen, M.; Nieminen, M. *Phys. Status Solidi A* **2004**, *201*, 1443. Zaera, F. *J. Mater. Chem.* **2008**, *18*, 3521. Kim, H.; Lee, H.-B.-R.; Maeng, W.-J. *Thin Solid Films* **2009**, *517*, 2563. Knez, M.; Nielsch, K.; Niinistö, L. *Adv. Mater.* **2007**, *19*, 3425.

(2) Rosenberg, R.; Edelstein, D. C.; Hu, C.-K.; Rodbell, K. P. *Annu. Rev. Mater. Sci.* **2000**, *30*, 229. Hau-Riege, C. S. *Microelectron. Reliab.* **2004**, *44*, 195. Kim, H. *Surf. Coat. Technol.* **2006**, *200*, 3104. Carraro, C.; Maboudian, R.; Magagnin, L. *Surf. Sci. Rep.* **2007**, *62*, 499. Shacham-Diamand, Y.; Inberg, A.; Sverdlov, Y.; Bogush, V.; Croitoru, N.; Moscovich, H.; Freeman, A. *Electrochim. Acta* **2003**, *48*, 2987.

(3) Vidjayacoumar, B.; Emslie, D. J. H.; Clendenning, S. B.; Blackwell, J. M.; Britten, J. F.; Rheingold, A. *Chem. Mater.* **2010**, DOI:10.1021/cm101442e.

Published on Web 08/11/2010

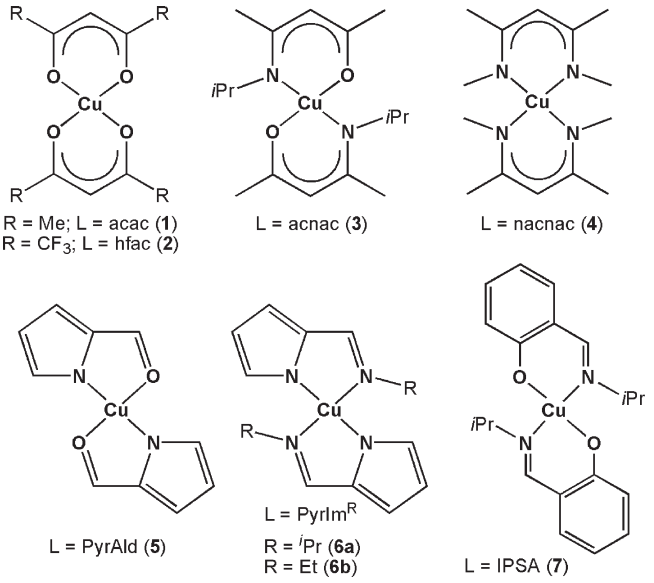

Figure 1. Homoleptic copper(II) complexes **1**−**7**.

N-ethyl-2-pyrrolylaldiminate ($PyrIm^{Et}$; **6b**) and *N*-isopropyl-2-salicylaldiminate (IPSA; **7**); Figure 1]. Solution reactions in this work provided a rapid and straightforward means to identify the most promising candidates for subsequent ALD/pulsed-CVD studies, which are much more time-consuming and resource intensive, and require the use of highly specialized equipment. On the basis of these studies, ALD/pulsed-CVD was attempted using **6b** in combination with BEt_3, $AlMe_3$, and $ZnEt_2$. No deposition was observed with BEt_3, consistent with much lower reactivity observed in solution, and although copper-containing films were deposited using $AlMe_3$ at 130 °C, they were nonconducting, presumably because of high Al_2O_3 content (after atmospheric exposure). However, with $ZnEt_2$, pulsed-CVD of conductive copper metal films (containing ~10 at % Zn) was achieved at 130 °C (lower temperatures were not accessible because of a minimum precursor delivery temperature of 120 °C). A related deposition process was reported by Sung and Fischer et al. during the course of this work; ALD of pure copper metal films using $[Cu(OCHMeCH_2NMe_2)_2]$ with $ZnEt_2$ at 100−120 °C.[4] However, these authors also encountered substantial Zn incorporation above 120 °C, presumably to the detriment of self-limiting behavior.

Beyond rapid screening of new metal precursor/coreagent combinations, solution reactions are amenable to detailed mechanistic study using a range of powerful characterization techniques, such as NMR spectroscopy and X-ray crystallography. By contrast, the direct study of ALD/pulsed-CVD mechanisms faces many challenges due to the very small quantities of surface and vapor-phase species involved, and metrology restrictions placed on chemical analysis inside an ALD reactor. Solution studies therefore represent a powerful approach to gain initial insight into the mechanisms behind ALD/pulsed-CVD processes, especially for reactions occurring at low temperature (e.g., < 150 °C); this insight can provide a starting-point for the development and study of new and improved ALD methods.

Solution studies have previously been employed for the study of CVD, and in a range of cases, comparison of volatile byproducts, deuterium labeling studies, and/or kinetic isotope effects have provided strong evidence for mechanistic parallels. For example: (1) Using $[Ti(CH_2{}^tBu)_4]$, both TiC CVD and solution thermolysis proceeded through initial α-hydrogen abstraction to release neopentane and form $[(^tBuCH_2)_2Ti{=}CH{}^tBu]$. Furthermore, in both fluorocarbon solution and the CVD process, this initial step was followed by further neopentane release via a mixture of α-hydrogen and γ-hydrogen abstraction pathways.[5] (2) For $[Pt(\kappa^1,\eta^2\text{-}CH_2CH_2CH_2CH{=}CH_2)_2]$, hot-tube CVD and solution studies yielded platinum metal and the same mixture of pentene and pentadiene products, consistent with the following reaction sequence: initial β-hydride elimination to yield 1,4-pentadiene and $[PtH(\kappa^1,\eta^2\text{-}CH_2CH_2CH_2CH{=}CH_2)]$, catalytic olefin isomerization by this hydride intermediate (conversion of 1,4-pentadiene to 1,3-pentadiene and 1-pentene to 2-pentene), and eventual reductive elimination to afford platinum and 1-pentene.[6] (3) In solution at room temperature, $[(fod)Pd(\eta^3\text{-}C_6H_9)]$ (fod = $^tBuCOCHCOC_3F_7$; C_6H_9 = 2-cyclohexenyl) decomposed to form a palladium mirror, benzene, cyclohexene and H(fod), consistent with initial β-hydride elimination to form [(fod)PdH] and 1,4-cyclohexadiene (free or bound), reductive elimination of H(fod) to yield palladium metal, and conversion of 1,4-cyclohexadiene to 1,3-cyclohexadiene and benzene at the palladium surface. Similarly, thermolysis of $[(fod)Pd(\eta^3\text{-}CH_2CMeCMe_2)]$ under CVD conditions with oxygen carrier gas gave palladium metal, H(fod) and $CH_2{=}CMe{-}CMe{=}CH_2$ as the major products, consistent with the same sequence of β-hydride elimination and reductive elimination.[7]

In this work, detailed spectroscopic investigations into the solution reactions of CuL_2 complex **6a** with $AlMe_3$, BEt_3, and $ZnEt_2$ are reported, allowing the principle pathways involved in copper metal deposition to be proposed. Reactions were monitored primarily by NMR spectroscopy, and intermediates and byproducts with appreciable thermal stability were synthesized independently to allow conclusive spectroscopic identification.

Results and Discussion

Copper(I) Intermediates En route to Copper Metal Deposition from 6a, 6b, or 7. In the screening reactions of copper(II) complexes **1**−**7** with $AlMe_3$, BEt_3, and $ZnEt_2$,[3] solution color changes were in many cases observed prior to metal deposition. This observation indicates disappearance of $[CuL_2]$ prior to metal deposition, rather than concurrent with metal deposition, and indeed a common diamagnetic intermediate was observed by ^1H NMR spectroscopy in the reactions of **6a**, **6b**, or **7** with ≤1 equiv. of $AlMe_3$, BEt_3, and $ZnEt_2$. These

(4) Lee, B. H.; Hwang, J. K.; Nam, J. W.; Lee, S. U.; Kim, J. T.; Koo, S.-M.; Baunemann, A.; Fischer, R. A.; Sung, M. M. *Angew. Chem., Int. Ed.* **2009**, *48*, 4536.

(5) Cheon, J.; Rogers, D. M.; Girolami, G. S. *J. Am. Chem. Soc.* **1997**, *119*, 6804. Entley, W. R.; Treadway, C. R.; Wilson, S. R.; Girolami, G. S. *J. Am. Chem. Soc.* **1997**, *119*, 6251.

(6) Tagge, C. D.; Simpson, R. D.; Bergman, R. G.; Hostetler, M. J.; Girolami, G. S.; Nuzzo, R. G. *J. Am. Chem. Soc.* **1996**, *118*, 2634.

(7) Zhang, Y. P.; Yuan, Z.; Puddephatt, R. J. *Chem. Mater.* **1998**, *10*, 2293.

Scheme 1. Generalized Reaction Scheme for the Formation of $[Cu^{I}_{x}L_{x}]$ as an Intermediate in the Reactions of $[Cu^{II}L_2]$ Complexes with $AlMe_3$, BEt_3 and $ZnEt_2$ (example shown here uses a pyrrolylaldimine precursor complex [e.g., 6a (R′ = ^{i}Pr) or 6b (R′ = Et)])[8]

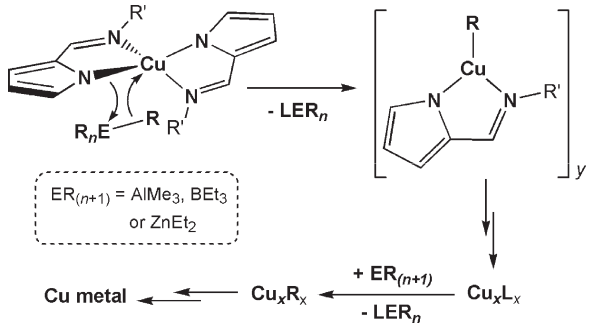

Scheme 2. Independent Synthesis of Complex 8

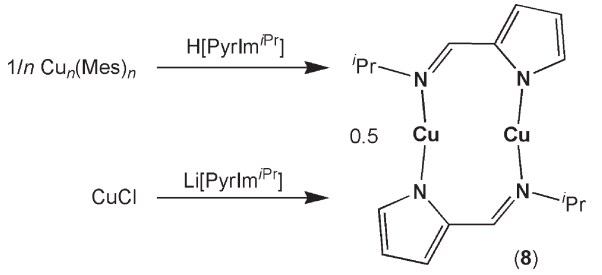

reactions are consistent with stepwise reduction via a copper(I) intermediate, $[Cu^{I}_{n}L_n]$, as shown in Scheme 1.[8]

The copper(I) intermediate formed in the reactions of **6a** with $AlMe_3$, BEt_3 and $ZnEt_2$ was synthesized independently from either mesitylcopper(I) with H[PyrIm^{iPr}] in toluene, or CuCl with Li[PyrIm^{iPr}] in THF (Scheme 2), and was identified as $[Cu_2(PyrIm^{iPr})_2]$ (**8**) by ^{1}H and ^{13}C NMR spectroscopy, combustion elemental analysis, and X-ray crystallography (Figure 2). In the solid state, complex **8** adopts a dinuclear structure reminiscent of Gordon's $[Cu_2(amidinate)_2]$ complexes.[9,10] However, in **8**, 4-atom bridges between the two copper(I) centers result in a nonplanar structure with approximate C_2 symmetry [N(1)−Cu(1)−Cu(2)−N(2) = 33.3(1)°; N(11)−Cu(2)−Cu(1)−N(12) = 31.4(1)°] and a longer Cu···Cu distance than in $[Cu_2\{(^{i}PrN)_2CMe\}_2]$ [2.5312(4) Å vs 2.424(1) Å].[10,11] The pyrrolyl nitrogen atom in **8** is nonplanar [cent−N(1)−Cu(1) = 168°; cent = centroid of N(1)/C(2)/C(3)/C(4)/C(5)], and Cu(1)−N(1) is only marginally shorter than Cu(2)−N(2) [1.866(2) Å vs 1.883(2) Å]. Significantly, nonplanar structures were also observed for several dinuclear copper(I) guanidinate complexes reported recently by Barry et al.[12]

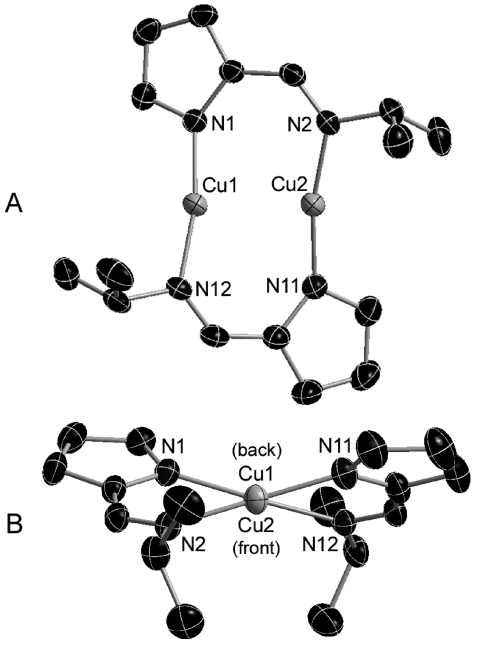

Figure 2. Solid-state structure of **8**·0.5toluene with thermal ellipsoids at 50% probability. All hydrogen atoms and solvent are omitted for clarity. Selected bond lengths (Å) and angles (deg): Cu(1)−N(1) = 1.866(2), Cu(2)−N(2) = 1.883(2), Cu(2)−N(11) = 1.863(2), Cu(1)−N(12) = 1.884(2), Cu(1)−Cu(2) = 2.5312(4), N(1)−Cu(1)−N(12) = 169.07(8), N(2)−Cu(2)−N(11) = 168.41(8).

In solution, complex **8** is stable for days, even at 120 °C. By contrast, other copper(I) intermediates in this work were much less stable; for example, the copper(I) complex observed in metal deposition reactions from $[Cu(IPSA)_2]$ (**7**) decomposed to copper metal over several hours in solution at room temperature. Observation of copper(I) intermediates in the reactions of **6a**, **6b** and **7** with $ZnEt_2$, $AlMe_3$ and BEt_3 highlights the potential for the formation of $[Cu^{I}_{x}L_{x}]$ complexes in situ during metal ALD, avoiding problems associated with the direct delivery of many copper(I) complexes because of low thermal stability.

Mechanistic Investigations. The reactions of **6a** with $AlMe_3$, BEt_3, and $ZnEt_2$ were studied by ^{1}H NMR spectroscopy over a range of temperatures with various copper precursor/ER_n coreagent ratios, and are discussed in detail below. The formation or absence of hydrogen, methane, ethane, ethylene,[13] and/or *n*-butane[14] was determined by comparison of ^{1}H and/or ^{13}C NMR chemical shifts with literature values (using gastight J. Young NMR tubes), and ^{1}H NMR after purging with argon gas. All other stable intermediates and byproducts in these reactions (Figure 3) were assigned by comparison with independently synthesized and characterized samples (vide infra).

Reactions of $[Cu(PyrIm^{iPr})_2]$ (6a) and $[Cu_2(PyrIm^{iPr})_2]$ (8) with $AlMe_3$. Reaction of dark-green, paramagnetic **6a** with 1.0 equiv. of $AlMe_3$ in C_6D_6 at room temperature resulted in immediate formation of a pale yellow solution and a small amount of a thermally unstable yellow precipitate.

(8) A copper(I) intermediate is likely in the reactions of all complexes (**1**−**7**) with $AlMe_3$, BEt_3, and $ZnEt_2$, but whether such a species can be observed spectroscopically depends on its thermal stability.
(9) Li, Z.; Barry, S. T.; Gordon, R. G. *Inorg. Chem.* **2005**, *44*, 1728. Lim, B. S.; Rahtu, A.; Gordon, R. G. *Nat. Mater.* **2003**, *2*, 749.
(10) Lim, B. S.; Rahtu, A.; Park, J.-S.; Gordon, R. G. *Inorg. Chem.* **2003**, *42*, 7951.
(11) The Cu−Cu distance in complex **8** could indicate the presence of a Cu−Cu interaction, especially given the extent to which the two copper centres bend towards one another [N(1)−N(2) 3.064 Å; Cu(1)−Cu(2) 2.531 Å; N(11)−N(12) 3.088 Å]. However, the subject of cuprophilic interactions has been one of some controversy: Hermann, H. L.; Boche, G.; Schwerdtfeger, P. *Chem.—Eur. J.* **2001**, *7*, 5333.
(12) Coyle, J. P.; Monillas, W. H.; Yap, G. P. A.; Barry, S. T. *Inorg. Chem.* **2008**, *47*, 683.
(13) Fulmer, G. R.; Miller, A. J. M.; Sherden, N. H.; Gottlieb, H. E.; Nudelman, A.; Stoltz, B. M.; Bercaw, J. E.; Goldberg, K. I. *Organometallics* **2010**, *29*, 2176.
(14) Abraham, R. J.; Warne, M. A.; Griffiths, L. *J. Chem. Soc. Perkin Trans. 2* **1997**, 31 and references therein .

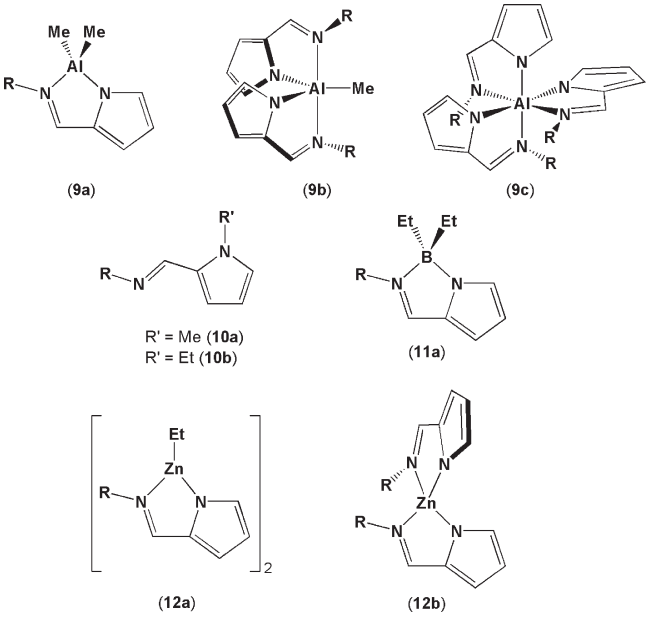

Figure 3. Pyrrolylaldimine ligand-containing byproducts ($R = {}^{i}$Pr) from the reactions of **6a** with $AlMe_3$, BEt_3, and $ZnEt_2$ (vide infra).

This precipitate was identified as $[CuMe]_n$[15,16] by reaction with $EtC(CH_2PPh_2)_3$ (triphos) to form soluble and thermally stable [(κ^3-triphos)CuMe], which was characterized by ^{1}H NMR spectroscopy in d_8-THF at 20 and −40 °C.[17] At room temperature, slurries of $[CuMe]_n$ in C_6D_6 or d^8-toluene (in the presence or absence of $AlMe_3$) decomposed over several hours to form finely divided copper metal and C_2H_6 (no methane was detected). Ikariya and Yamamoto reported the clean formation of ethane from slow decomposition of dry $[CuMe]_n$ at 0 °C[18] or phosphine-stabilized [(Cy_3P)CuMe].[19,20] However, these and other researchers reported the formation of both methane and ethane in the rapid or explosive decomposition of solid $[CuMe]_n$, with[18,19,21] or without[15] the formation of small amounts of ethylene and hydrogen or propane. Release of methane and ethane was also reported for the thermal decomposition of various [$(R_3P)_x$CuMe] [$(R_3P)_x$ = PEt_3, P^nBu_3, PMe_2Ph, dppe, $(PPh_3)_3$] complexes.[20]

After 15 min, a ^{1}H NMR spectrum of the 1:1 reaction of **6a** with $AlMe_3$ showed the formation of [Cu_2(PyrIm$^{i\mathrm{Pr}}$)$_2$] (**8**), [(PyrIm$^{i\mathrm{Pr}}$)$AlMe_2$] (**9a**), PyrIm$^{i\mathrm{Pr}}$-Me (**10a**), ethane and a small amount of [(PyrIm$^{i\mathrm{Pr}}$)$_2$AlMe] (**9b**). No $AlMe_3$ remained, and complete consumption of **6a** was evident by the absence of a broad ^{1}H NMR peak at 3.2 ppm, and a pale yellow solution color (**6a** is dark green). The primary route to **9a** must therefore be the reaction of $AlMe_3$ with **6a**, with **9b** formed subsequently in the reaction of **9a** with **8**. On the basis of the observed product distribution, the intermediate copper alkyl complexes, "(PyrIm$^{i\mathrm{Pr}}$)CuMe" and $[CuMe]_n$, must decompose to afford **8** [with loss of ethane or **10a**] and copper metal [with loss of ethane], respectively (Scheme 3); the reactions responsible for **10a** formation are discussed further below. Over the next 48 h at room temperature, deposition of a copper film occurred on the walls of the NMR tube, and ^{1}H NMR signals for **9b** grew in intensity at the expense of those for **8** and **9a**. A small amount of a new byproduct, [Al(PyrIm$^{i\mathrm{Pr}}$)$_3$] (**9c**), was also formed. No further changes were observed even after 24 h at 100 °C.

Scheme 3. Reaction Pathways Responsible for Copper Metal Deposition from 6a and 8 with $AlMe_3$ (L = PyrIm$^{i\mathrm{Pr}}$)[a]

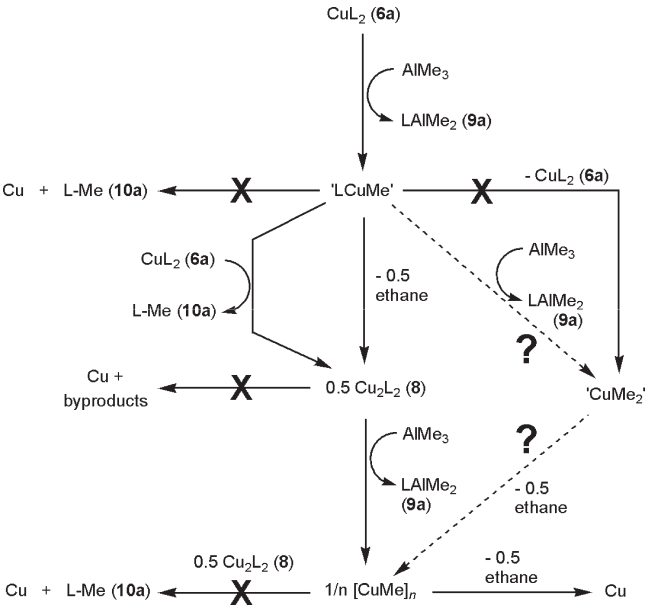

[a] Reactions marked with an X do not occur. Dotted arrows represent reactions that cannot be ruled out in the presence of a large excess of $AlMe_3$.

Reactions of **6a** with an excess or deficit of $AlMe_3$ were also investigated. Such conditions are relevant to ALD/pulsed-CVD process development where reaction stoichiometry is dependent on precursor and coreactant pulse durations. In comparison to the 1:1 reaction of **6a** with $AlMe_3$, which deposited a copper film slowly over several days at room temperature, the 1:5 reaction resulted in immediate formation of a bright yellow precipitate of $[CuMe]_n$, and only [(PyrIm$^{i\mathrm{Pr}}$)$AlMe_2$] (**9a**), ethane and remaining $AlMe_3$ were observed in solution. Formation of these products requires rapid reaction of $AlMe_3$ with **6a**, and subsequent reaction of $AlMe_3$ with either in situ generated "(PyrIm$^{i\mathrm{Pr}}$)CuMe" or [Cu_2(PyrIm$^{i\mathrm{Pr}}$)$_2$] (**8**).

A ^{1}H NMR spectrum of the 1:0.5 reaction of **6a** with $AlMe_3$ taken after 15 min showed formation of [Cu_2(PyrIm$^{i\mathrm{Pr}}$)$_2$] (**8**), [(PyrIm$^{i\mathrm{Pr}}$)$AlMe_2$] (**9a**), PyrIm$^{i\mathrm{Pr}}$-Me (**10a**), ethane, and leftover **6a** (Figure 4). No copper metal or other precipitate was observed, and as expected, no $AlMe_3$ remained unreacted. After 4 h, all **6a** had been

(15) Gilman, H.; Jones, R. G.; Woods, L. A. *J. Org. Chem.* **1952**, *17*, 1630.
(16) $[CuMe]_n$ and related phosphine adducts have been prepared by reaction of [Cu(acac)$_2$] with $AlMe_2$(OMe) or $AlMe_2$(O^{i}Pr) in the presence or absence of a phosphine ligand: (a) Ikariya, T.; Yamamoto, A. *J. Organomet. Chem.* **1974**, *72*, 145. (b) Pasynkiewicz, S.; Poplawska, J. *J. Organomet. Chem.* **1985**, *282*, 427. (c) Coan, P. S.; Folting, K.; Huffman, J. C.; Caulton, K. G. *Organometallics* **1989**, *8*, 2724.
(17) Coan, P. S.; Folting, K.; Huffman, J. C.; Caulton, K. G. *Organometallics* **1989**, *8*, 2724.
(18) Ikariya, T.; Yamamoto, A. *J. Organomet. Chem.* **1974**, *72*, 145.
(19) Pasynkiewicz, S.; Poplawska, J. *J. Organomet. Chem.* **1985**, *282*, 427.
(20) Miyashita, A.; Yamamoto, T.; Yamamoto, A. *Bull. Chem. Soc. Jpn.* **1977**, *50*, 1109.
(21) Pasynkiewicz, S.; Poplawska, J. *J. Organomet. Chem.* **1986**, *302*, 269.

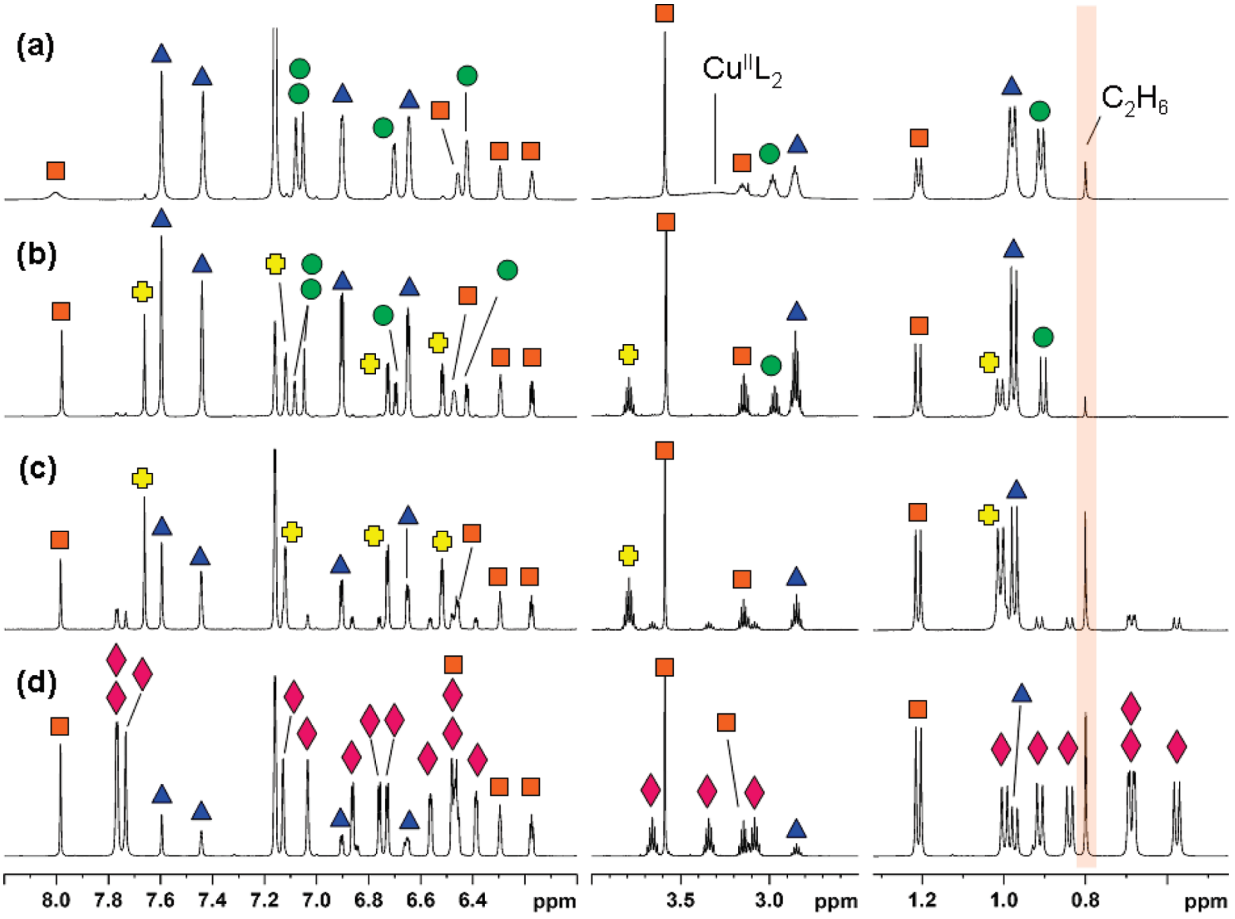

Figure 4. Selected regions of the 500 MHz ^{1}H NMR spectra for the 1:0.5 reaction of **6a** with $AlMe_3$ in C_6D_6: (a) 15 min at 20 °C, (b) 4 h at 20 °C, (c) 3 days at 20 °C, (d) 3 days at 20 °C followed by 2 days at 60 °C. In spectra a−c, the AlCH_3 peak for **9a** and **9b** (−0.32 ppm) is not shown. The shaded area highlights the chemical shift position of ethane. Symbols mark different reaction intermediates and byproducts: triangle (blue) = [Cu_2(PyrIm)$_2$] (**8**), circle (green) = [(PyrIm)$AlMe_2$] (**9a**), cross (yellow) = [(PyrIm)$_2$AlMe] (**9b**), diamond (purple) = [Al(PyrIm)$_3$] (**9c**), square (orange) = PyrIm-Me (**10a**).

consumed, despite the release of only 0.3 equiv. of **9a** and 0.2 equiv. of [(PyrIm)$_2$AlMe] (**9b**). Equation 1 shows the major products formed in this reaction

$$\begin{aligned} &CuL_2\ (\mathbf{6a}) + 0.5\ AlMe_3 \rightarrow 0.5\ Cu_2L_2\ (\mathbf{8}) \\ &+ 0.3\ LAlMe_2\ (\mathbf{9a}) + 0.2\ L_2AlMe + 0.3\ L{-}Me\ (\mathbf{10a}) \\ &+ 0.2\ C_2H_6 \end{aligned} \quad (1)$$

$$\begin{aligned} &CuL_2\ (\mathbf{6a}) + 0.5\ AlMe_3 \rightarrow 0.5\ CuL_2\ (\mathbf{6a}) \\ &+ 0.5\ LAlMe_2\ (\mathbf{9a}) + 0.5\ \text{“LCuMe”} \end{aligned} \quad (2)$$

$$\begin{aligned} &x\ \text{“LCuMe”} + x\ CuL_2\ (\mathbf{6a}) \rightarrow x\ Cu_2L_2\ (\mathbf{8}) + x\ L{-}Me\ (\mathbf{10a}) \\ &[x = 0.3\ \text{in the 1:0.5 Cu:Al reaction}] \end{aligned} \quad (3)$$

$$\begin{aligned} &y\ \text{“LCuMe”} \rightarrow 0.5y\ Cu_2L_2\ (\mathbf{8}) + 0.5y\ \text{ethane} \\ &[y = 0.2\ \text{in the 1:0.5 Cu:Al reaction}] \end{aligned} \quad (4)$$

The 1:1 ratio of [Cu_2(PyrIm$^{i\text{Pr}}$)$_2$] (**8**) to PyrIm$^{i\text{Pr}}$-Me (**10a**), absence of leftover **6a**, and only small amounts of ethane and [(PyrIm$^{i\text{Pr}}$)$_2$AlMe] (**9b**) observed under these conditions imply a mechanism in which “(PyrIm$^{i\text{Pr}}$)CuMe” is formed via eq 2, and reacts with remaining **6a** to form **8** and **10a**, as shown in eq 3. Equation 3 is therefore the dominant pathway en route to complex **8** in the 1:0.5 reaction of **6a** with $AlMe_3$. By contrast, in the 1:1 reaction of **6a** with $AlMe_3$ (vide supra), eq 3 accounts for approximately 30% of complex **8** formed, and elimination of ethane from “(PyrIm$^{i\text{Pr}}$)CuMe” (eq 4) accounts for the other 70%. The formation of **10a** presumably occurs via bimolecular C−N bond forming reductive elimination, since it is not accompanied by copper metal deposition. This reactivity is quite unusual; for example, it lies outside of the range of mechanisms typically proposed for copper-catalyzed C−N bond forming Ullmann reactions.[22]

Over 72 h at room temperature, the 1:0.5 reaction of **6a** with $AlMe_3$ resulted in deposition of a copper mirror, formation of a significant quantity of ethane, and an approximate 3:3:1:2 ratio of PyrIm$^{i\text{Pr}}$-Me (**10a**), [(PyrIm$^{i\text{Pr}}$)$_2$AlMe] (**9b**), [Al(PyrIm$^{i\text{Pr}}$)$_3$] (**9c**), and [Cu_2(PyrIm$^{i\text{Pr}}$)$_2$] (**8**) (Figure 4). Subsequent heating at 60 °C for 48 h effected complete conversion to **10a**, copper metal, ethane, and **9c**, with only 0.075 equiv. of dinuclear **8** remaining (Figure 4).[23]

(22) Monnier, F.; Taillefer, M. *Angew. Chem., Int. Ed.* **2009**, *48*, 6954. Evano, G.; Blanchard, N.; Toumi, M. *Chem. Rev.* **2008**, *108*, 3054. Tye, J. W.; Weng, Z.; Johns, A. M.; Incarvito, C. D.; Hartwig, J. F. *J. Am. Chem. Soc.* **2008**, *130*, 9971. Strieter, E. R.; Bhayana, B.; Buchwald, S. L. *J. Am. Chem. Soc.* **2009**, *131*, 78.

(23) Complex **9c** also formed in small amounts after 3 days at room temperature.

Reaction of isolated [$Cu_2(PyrIm^{iPr})_2$] (**8**) with 1−5 equiv. of $AlMe_3$ resulted in precipitation of $[CuMe]_n$ and formation of [$(PyrIm^{iPr})AlMe_2$] (**9a**) as the only soluble byproduct. By contrast, reaction of **8** with 0.5 equiv. of $AlMe_3$ resulted in precipitation of $[CuMe]_n$, leaving a 1:1 mixture of **9a** and remaining **8**. Complex **8** was then consumed over 48 h to give a copper mirror, ethane, and a mixture of **9a**, [$(PyrIm^{iPr})_2$-AlMe] (**9b**) and [$Al(PyrIm^{iPr})_3$] (**9c**). The C−N coupling product $PyrIm^{iPr}$-Me (**10a**) was not observed in any reactions of **8** with $AlMe_3$.

Scheme 3 shows reaction pathways for copper deposition from [$Cu(PyrIm^{iPr})_2$] (**6a**) and [$Cu_2(PyrIm^{iPr})_2$] (**8**) with $AlMe_3$. Reactions marked with an "X", can be ruled out based on the following arguments: (1) Formation of copper metal from thermal decomposition of [$Cu_2(PyrIm^{iPr})_2$] (**8**) does not occur; complex **8** is thermally stable in solution for days at 120 °C. (2) Decomposition of "$(PyrIm^{iPr})CuMe$" to form $PyrIm^{iPr}$-Me (**10a**) and copper metal does not occur; $PyrIm^{iPr}$-Me is formed only in reactions with low $AlMe_3$ stoichiometries, and is formed in the absence of Cu metal deposition. Furthermore, the ratio of (**9a**+**9b**+**9c**) to L−Me remains constant after all **6a** has been consumed. (3) On the basis of observed product distributions, decomposition of "$(PyrIm^{iPr})CuMe$" to form **10a** without consumption of **6a** does not occur. (4) Ligand redistribution from "$(PyrIm^{iPr})$-CuMe" to form **6a** and "$CuMe_2$" does not occur because "$CuMe_2$" would provide access to $[CuMe]_n$ and/or copper metal without the intermediacy of **8**, a pathway that is not supported by observed product distributions. (5) Reaction of $[CuMe]_n$ with **8** to form **10a** and copper metal can be ruled out because reactions of **8** with $AlMe_3$ do not provide **10a**.

The major reactions responsible for copper metal deposition (Scheme 3) are therefore: (1) Reaction of **6a** with $AlMe_3$ to form "$(PyrIm^{iPr})CuMe$". (2) Decomposition of "$(PyrIm^{iPr})CuMe$" by reaction with **6a** to eliminate $PyrIm^{iPr}$-Me (**10a**) (at low $AlMe_3$ reaction stoichiometries) or bimolecular reductive elimination of ethane (at higher $AlMe_3$ stoichiometries);[24] both pathways yield [$Cu_2(PyrIm^{iPr})_2$] (**8**). (3) Reaction of **8** with $AlMe_3$ to form $[CuMe]_n$. (4) Decomposition of $[CuMe]_n$ (to form only ethane in C_6D_6 or d_8-toluene) via bimolecular reductive elimination. However, in reactions of **6a** with a significant excess of $AlMe_3$, the intermediacy of "$CuMe_2$" en route to "CuMe" cannot be ruled out (vide infra).

Reactions of [$Cu(PyrIm^{iPr})_2$] (6a) and [$Cu_2(PyrIm^{iPr})_2$] (8) with BEt_3. Complex **6a** reacted with 0.5 to 1.0 equiv. of BEt_3 over 10 weeks at room temperature to form a 1:1:1 mixture of [$Cu_2(PyrIm^{iPr})_2$] (**8**), $PyrIm^{iPr}$-Et (**10b**), and [$(PyrIm^{iPr})BEt_2$] (**11a**) The absence of copper metal or volatile byproducts (ethylene, ethane, *n*-butane, or H_2) in this reactivity rules out direct decomposition of "$(PyrIm^{iPr})$-CuEt" to give Cu metal and **10b**, as well as any mechanism involving "$CuEt_2$" formation. The observed product distribution is however consistent with the initial formation of '$(PyrIm^{iPr})CuEt$', and subsequent reaction with **6a** to eliminate **10b**

Scheme 4. Reaction Pathway for Copper Metal Deposition from 6a and 8 with BEt_3 at 100 °C (L = $PyrIm^{iPr}$)[a]

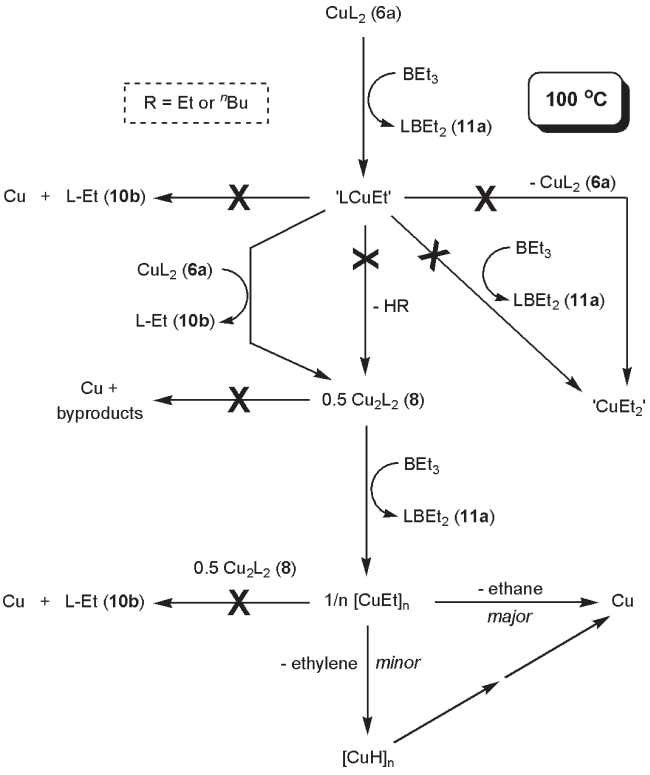

[a] Reactions marked with an X do not occur.

in preference to bimolecular reductive elimination of *n*-butane or β-hydride elimination to release ethylene. Identical reactivity was observed with 5.0 equiv. of BEt_3 at 100 °C for 3 h.

At room temperature, isolated dinuclear [$Cu_2(PyrIm^{iPr})_2$] (**8**) reacted only very slowly with BEt_3. However, at 100 °C, the reaction of **8** with BEt_3 (10 equiv.) was complete after 24 h, cleanly forming a copper mirror, [$(PyrIm^{iPr})BEt_2$] (**11a**), ethane, and a very small amount of ethylene (hydrogen or $PyrIm^{iPr}$-Et (**10b**) formation was not observed; see Figure S1 in the Supporting Information). The nature of these byproducts is suggestive of initial "CuEt" formation, with decomposition at 100 °C taking place primarily by bond homolysis and a small amount of β-hydride elimination. The preference for bond homolysis likely arises due to slow formation of "CuEt" (as a consequence of the greatly reduced reactivity of **8** with BEt_3, relative to $AlMe_3$), leading to very low concentrations of "CuEt" (and "CuH" via β-hydride elimination) in solution, which would disfavor bimolecular reactivity, such as reductive elimination of H_2 or *n*-butane. Pathways responsible for copper metal deposition in the reactions of **6a** and **8** with BEt_3 are summarized in Scheme 4. The significantly lower reactivity of BEt_3 relative to $AlMe_3$ (and $ZnEt_2$; vide infra) may be attributed to the reduced Lewis acidity of trialkylboranes relative to trialkylalanes,[25] an increase in E−C bond strength in the order Zn < Al < B,[26] and reduced bond polarity[27] (pauling electronegativity values: C = 2.55, B = 2.04, Al = 1.61, Zn = 1.65).[26]

(24) Reactions of **6a** or **8** with 5 equiv. of $AlMe_3$ or $ZnEt_2$ in d_8-toluene formed exactly the same mixtures of products observed in C_6D_6, indicative of copper reduction via reductive elimination rather than bond homolysis pathways.

(25) Housecroft, C. E.; Sharpe, A. G. *Inorganic Chemistry*, 2nd ed.; Pearson Education: Harlow, U.K., 2005.
(26) Shriver, D. F.; Atkins, P. W.; Langford, C. H., *Inorganic Chemistry*, 2nd ed.; Oxford University Press: Oxford, U.K., 1994.
(27) Köster, R.; Binger, P. *Adv. Inorg. Chem. Radiochem.* **1965**, *7*, 263.

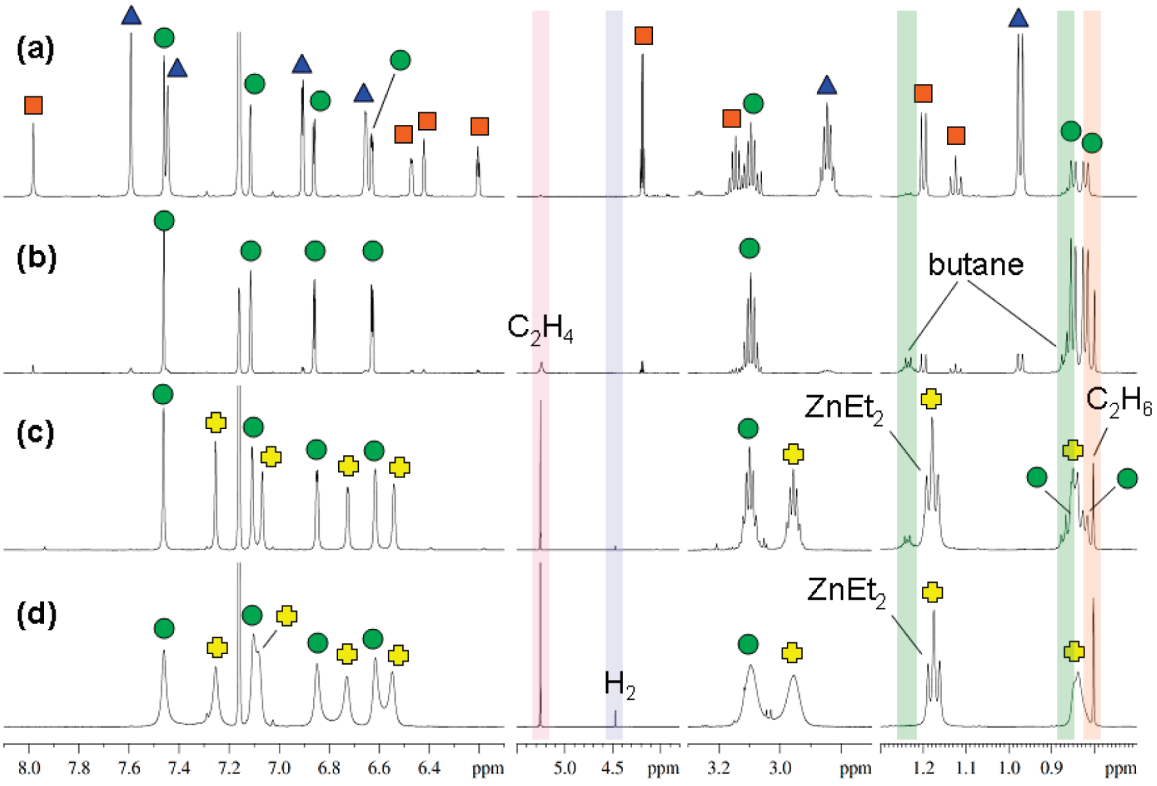

Figure 5. Selected regions of the 600 MHz ^{1}H NMR spectra for reactions between **6a** or **8** with $ZnEt_2$ at 20 °C in C_6D_6: (a) **6a** + 0.3 equiv. of $ZnEt_2$ after 15 min, (b) **6a** + 1 equiv. of $ZnEt_2$ after 15 min, (c) **6a** + 5 equiv. of $ZnEt_2$ after 1 h, (d) **8** + 5 equiv. of $ZnEt_2$ after 15 min. In spectra c and d, the $ZnCH_2$ peak (0.18 ppm) for ethyl groups exchanging between [(PyrIm^{iPr})ZnEt] and $ZnEt_2$ (vide infra) is not shown. Shaded areas highlight chemical shift positions for gaseous byproducts (H_2, ethylene, ethane, and *n*-butane). Symbols mark different reaction intermediates and byproducts: triangle (blue) = [Cu_2(PyrIm^{iPr})$_2$] (**8**), square (orange) = PyrIm^{iPr}-Et (**10b**), cross (yellow) = [(PyrIm^{iPr})ZnEt] (**12a**), circle (green) = [Zn(PyrIm^{iPr})$_2$] (**12b**).

Reactions of [Cu(PyrIm^{iPr})$_2$] (6a) and [Cu_2(PyrIm^{iPr})$_2$] (8) with $ZnEt_2$. At room temperature, complex **6a** reacted immediately with 0.3 equiv. of $ZnEt_2$ to form an orange solution that turned pale yellow over a period of ~1 min. This reaction proceeded cleanly to form a 0.5:0.4:0.3 mixture of [Cu_2(PyrIm^{iPr})$_2$] (**8**), PyrIm^{iPr}-Et (**10b**), and [Zn(PyrIm^{iPr})$_2$] (**12b**), and was accompanied by the formation of a small amount of *n*-butane (spectrum a in Figure 5), but no copper metal. Ethylene was not detected, indicating that β-hydride elimination from "(PyrIm^{iPr})-CuEt" does not occur to any significant extent. Equation 5 provides the overall stoichiometry of the reaction, which is consistent with the reaction steps presented in eqs 6−8.

$$[CuL_2]\ (\mathbf{6a}) + 0.3\ ZnEt_2 \rightarrow 0.5\ [Cu_2L_2]\ (\mathbf{8}) + 0.3\ [ZnL_2](12\mathbf{b}) + L{-}Et\ (\mathbf{10b}) \quad (5)$$

$$[CuL_2]\ (\mathbf{6a}) + 0.3\ ZnEt_2 \rightarrow 0.4\ [CuL_2]\ (\mathbf{6a}) + 0.3\ [ZnL_2]\ (\mathbf{12b}) + 0.6\ \text{"LCuEt"} \quad (6)$$

$$0.4\ [CuL_2]\ (\mathbf{6a}) + 0.4\ \text{"LCuEt"} \rightarrow 0.4\ [Cu_2L_2]\ (\mathbf{8}) + 0.4\ L{-}Et\ (\mathbf{10b}) \quad (7)$$

$$0.2\ \text{"LCuEt"} \rightarrow 0.1\ [Cu_2L_2]\ (\mathbf{8}) + 0.1\ n\text{-butane} \quad (8)$$

By contrast, reaction of **6a** with 0.5 equiv. of $ZnEt_2$ afforded an orange solution from which a black precipitate of copper metal was deposited over ~1 min. Byproducts in this reaction were [Cu_2(PyrIm^{iPr})$_2$] (**8**), [Zn(PyrIm^{iPr})$_2$] (**12b**), and PyrIm^{iPr}-Et (**10b**) in a 0.4:0.5:0.2 ratio, *n*-butane, ethylene, and ethane. The overall stoichiometry of these reactions is shown in eq 9, which may be explained through the series of reactions in eqs 10−14 (note: *n*-butane is not formed in reactions of **8** with $ZnEt_2$; vide infra). Similar observations were made with 1.0 equiv. of $ZnEt_2$ (spectrum b in Figure 5), although in this case, only very small amounts of **8** and **10b** were present. Upon increasing the amount of $ZnEt_2$ to 5.0 equiv., complexes **8** and **10b** disappeared from the product mixture, [(PyrIm^{iPr})ZnEt] (**12a**) was now observed (in equilibrium with **12b** and $ZnEt_2$; vide infra), and a small amount of hydrogen was also produced (spectrum c in Figure 5). In the latter reaction, the absence of **10b** as a reaction product is consistent with rapid **6a** depletion (due to fast reaction with excess $ZnEt_2$), rendering **6a** unavailable for reaction with in situ generated "(PyrIm^{iPr})CuEt" (cf. eq 11), and the absence of **8** is readily explained by reaction of **8** with remaining $ZnEt_2$ (as in eq 13). However, an alternative route to copper metal that circumvents complex **8** is the reaction of in situ generated "(PyrIm^{iPr})CuEt" with $ZnEt_2$ to form "$CuEt_2$", rather than decomposition of "(PyrIm^{iPr})-CuEt" by *n*-butane elimination or reaction with **6a**. The resulting "$CuEt_2$" species would undoubtedly be highly unstable, decomposing to copper metal directly or through

the intermediacy of "CuEt" (vide infra).

$$CuL_2\ (\mathbf{6a}) + 0.5\ ZnEt_2 \rightarrow 0.4\ Cu_2L_2\ (\mathbf{8}) + 0.2\ Cu + 0.5\ ZnL_2\ (\mathbf{12b}) + 0.2\ L{-}Et\ (\mathbf{10b}) + x\ C_4H_{10} + y\ C_2H_4 + y\ C_2H_6 \quad (9)$$

$$CuL_2\ (\mathbf{6a}) + 0.4\ ZnEt_2 \rightarrow 0.2\ CuL_2\ (\mathbf{6a}) + 0.4\ ZnL_2\ (\mathbf{12b}) + 0.8\ \text{"LCuEt"} \quad (10)$$

$$0.2\ CuL_2\ (\mathbf{6a}) + 0.2\ \text{"LCuEt"} \rightarrow 0.2\ Cu_2L_2\ (\mathbf{8}) + 0.2\ L{-}Et\ (\mathbf{10b}) \quad (11)$$

$$0.6\ \text{"LCuEt"} \rightarrow 0.3\ Cu_2L_2\ (\mathbf{8}) + 0.3\ n\text{-butane} \quad (12)$$

$$0.1\ Cu_2L_2\ (\mathbf{8}) + 0.1\ ZnEt_2 \rightarrow 0.1\ ZnL_2\ (\mathbf{12b}) + 0.2\ \text{"CuEt"} \quad (13)$$

$$0.2\ \text{"CuEt"} \rightarrow 0.2\ Cu + 0.2\ C_2H_4 + 0.2\ C_2H_6 \quad (14)$$

The isolated copper(I) intermediate $[Cu_2(PyrIm^{iPr})_2]$ (**8**) reacted instantly with 1.0 or 5.0 equiv. of $ZnEt_2$ (spectrum d in Figure 5) to form $[(PyrIm^{iPr})ZnEt]$ (**12a**) and/or $[Zn(PyrIm^{iPr})_2]$ (**12b**), and to deposit a thermally unstable bright orange powder that decomposed to copper metal in <1 min at room temperature. This unstable orange powder is presumably $[CuEt]_n$, by analogy with $[CuMe]_n$. Volatile byproducts of the reaction between **8** and $ZnEt_2$ are ethane, ethylene, and small amounts of H_2 (*n*-butane was not formed), consistent with $[CuEt]_n$ decomposition by β-hydrogen elimination and reductive elimination.[24] This decomposition mode for $[CuEt]_n$ contrasts that observed in reactions of **8** with BEt_3, presumably because $[CuEt]_n$ is generated at room temperature, rather than at 100 °C in reactions with BEt_3, and in significantly higher concentrations (due to the much greater reactivity of $ZnEt_2$ compared with BEt_3). A compound formulated as $[CuEt]_n$ has previously been prepared in the reactions of (1) CuI with EtMgBr in OEt_2,[15] and (2) CuCl with EtMgBr in THF,[28] and in both cases was reported to decompose readily by β-hydride elimination of ethylene and subsequent reductive elimination of ethane and hydrogen. Analogous reactivity has also been reported for $[Cu^nPr]_n$ and $[Cu^nBu]_n$,[28] as well as phosphine-coordinated $[(R'_3P)_xCuR]$ (R = Et, ^{n}Pr, ^{n}Bu, or ^{i}Bu; $R'_3P = PPh_3$, PCy_3, or P^nBu_3) complexes.[18,20,29]

The NMR studies outlined above are consistent with the following sequence of reactions for copper metal deposition from $[Cu(PyrIm^{iPr})_2]$ (**6a**) with $ZnEt_2$ (Scheme 5): (1) Reaction of **6a** with $ZnEt_2$ to form "$(PyrIm^{iPr})CuEt$" and $[(PyrIm^{iPr})ZnEt]$ (**12a**) or $[Zn(PyrIm^{iPr})_2]$ (**12b**). (2) Decomposition of "$(PyrIm^{iPr})CuEt$" by reaction with **6a** to eliminate $PyrIm^{iPr}$-Et (**10b**) (at low $ZnEt_2$ reaction stoichiometries) or bimolecular reductive elimination of *n*-butane (at higher $ZnEt_2$ stoichiometries); both pathways provide access to $[Cu_2(PyrIm^{iPr})_2]$ (**8**). (3) Reaction of **8** with $ZnEt_2$ to form "CuEt". (4) β-Hydride elimination of ethylene from $[CuEt]_n$ to form "CuH". (5) Decomposition of "CuH" via binuclear reductive elimination of ethane (major product via reaction of "CuH" with "CuEt") or hydrogen (minor product formed from 2 molecules of "CuH"). However, as discussed above, the intermeciacy of "$CuEt_2$" cannot be ruled out at higher $ZnEt_2$ stoichiometries; this possibility is discussed further below.

Scheme 5. Reaction Pathways for Copper Metal Deposition from 6b with $ZnEt_2$ (L = $PyrIm^{iPr}$)[a]

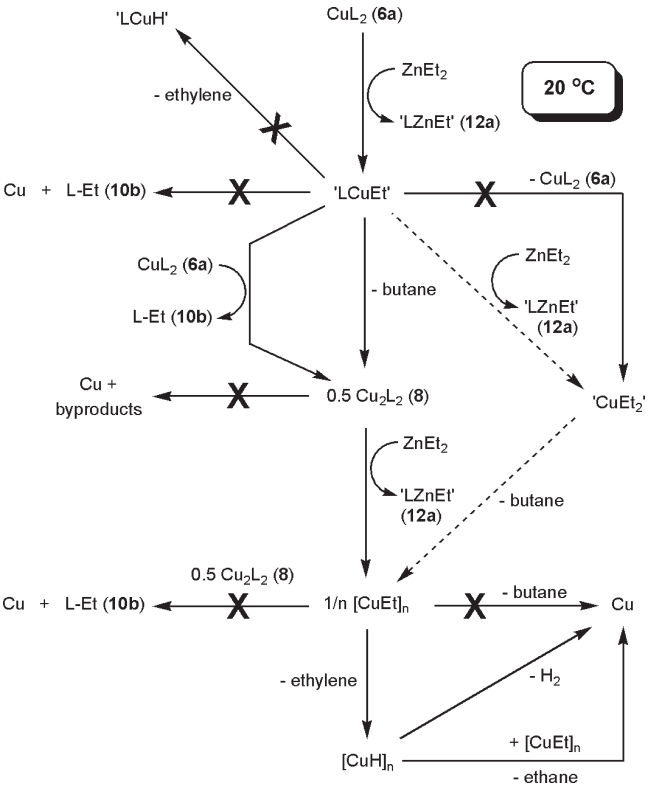

[a] Reactions marked with an X do not occur. Dotted arrows represent reactions that cannot be ruled out in the presence of a large excess of $ZnEt_2$.

Possible Intermediacy of a Dialkylcopper(II) Species in the Reactions of CuL_2 (6a) with Excess $AlMe_3$ or $ZnEt_2$. On the basis of the experiments described above, it is not possible to rule out the intermediacy of "CuR_2" (R = Me or Et) in the reactions of **6a** with a large excess of $AlMe_3$ or $ZnEt_2$. The accessibility of "$(PyrIm^{iPr})CuR$" for reaction with **6a** or "$(PyrIm^{iPr})CuR$" (resulting in $PyrIm^{iPr}$-R or R_2 elimination, respectively) demonstrates some persistance of "$(PyrIm^{iPr})CuR$" in solution, making the reaction of "$(PyrIm^{iPr})CuR$" with excess $AlMe_3$ or $ZnEt_2$ at least feasible. This is particularly the case for $AlMe_3$ and $ZnEt_2$, given the observed order of reactivity: $ZnEt_2 \approx AlMe_3 \gg BEt_3$.

To further investigate the potential intermediacy of "CuR_2" (R = Me or Et), the reactions of **6a** with 5 equiv. of $AlMe_3$ and $ZnEt_2$ were investigated in d_8-toluene at -80 °C in the presence of $O(SiMe_3)_2$ as an internal standard for integration.[24] The low temperature ^{1}H NMR spectrum of the $AlMe_3$ reaction (generated in situ at -80 °C and maintained at this temperature) showed release of 2 equivalents of $[(PyrIm^{iPr})AlMe_2]$ (**9a**) per equivalent of **6a** consumed.

(28) Wada, K.; Tamura, M.; Kochi, J. *J. Am. Chem. Soc.* **1970**, *92*, 6656.
(29) Whitesides, G. M.; Stedronsky, E. R.; Casey, C. P.; San Filippo, J. J. *J. Am. Chem. Soc.* **1970**, *92*, 1426.

However, a significant quantity of ethane was also detected (comparable with identical reactions conducted at room temperature), indicating that reduction to copper(I) had already occurred. Furthermore, broad signals suggestive of a paramagnetic copper(II) complex were conspicuously absent from the ^{1}H NMR spectrum, and the only species[30] detected in solution were [(PyrIm$^{i\mathrm{Pr}}$)AlMe$_2$] [δ −0.16 (s, Al*Me*)] and (AlMe$_3$)$_2$ [δ 0.00 (s, 6H, μ-*Me*), −0.52 (s, 12H, *Me*)]. Similar observations were made in low-temperature reactions of **6a** with ZnEt$_2$. These reactions also show that only *n*-butane (not ethylene or ethane) is produced when reactions of **6a** with excess ZnEt$_2$ are maintained below −20 °C where [CuEt]$_n$ is stable (very rapid ethylene evolution was observed upon warming the reaction above 10 °C).

Dialkyl copper(II) intermediates ("CuR$_2$") remain viable intermediates en route to "CuR", especially in the presence of a large excess of AlMe$_3$ or ZnEt$_2$. However, given that reduction to copper(I) proceeds rapidly, even at −80 °C, this possibility was not investigated further. The thermal instability of copper(II) alkyl complexes is well documented. For example, reaction of CuCl$_2$ with RMgBr (R = Me or Et), MgMe$_2$ or MeLi has been reported to yield only the copper(I) alkyl product [CuR]$_n$ and R$_2$ (ethane or *n*-butane), presumably via in situ generated "ClCuR" or "CuR$_2$".[15,28] Similarly, reaction of LiCu^{n}Bu$_2$ with O$_2$ or nitrobenzene was reported to yield [Cu^{n}Bu]$_n$ with *n*-octane as the primary byproduct,[31] and oxidation of [(NHC)CuR] (R = Me or Et) with AgOTf resulted in rapid formation of [(NHC)Cu(OTf)] and R$_2$ (ethane or *n*-butane) through a mechanism which does not involve alkyl group transfer to silver(I), and does not appear to involve alkyl radicals.[32] However, it is of note that several instances of copper(II) alkyl species with appreciable stability have appeared in the recent literature. For example, the copper(II) complexes [(κ^4*CN*$_3$-C(S−C$_5$H$_4$N)$_3$}CuX] (X = F, Cl, Br, I),[33] [(κ^4*CN*$_3$-C(S−C$_5$H$_4$N)$_3$}Cu(NCMe)][PF$_6$][34] and [(NCP)Cu] (NCP = N-confused porphyrin)[35] were isolated as stable solids, and an electrochemical study of [Cu$_2${μ:κ^2*CN*-C(SiMe$_3$)$_2$(C$_5$H$_4$N)}$_2$] revealed reversible oxidation to a cationic copper(II) alkyl species in solution.[36]

Independent Synthesis and Characterization of Byproducts from Copper Deposition Studies. The complexes [(PyrIm$^{i\mathrm{Pr}}$)AlMe$_2$] (**9a**), [(PyrIm$^{i\mathrm{Pr}}$)$_2$AlMe] (**9b**), [Al(PyrIm$^{i\mathrm{Pr}}$)$_3$] (**9c**), [(PyrIm$^{i\mathrm{Pr}}$)BEt$_2$] (**11a**), [(PyrIm$^{i\mathrm{Pr}}$)ZnMe] (**12a**) and [Zn(PyrIm$^{i\mathrm{Pr}}$)$_2$] (**12b**) (Figure 3) were prepared by reaction of H[PyrIm$^{i\mathrm{Pr}}$] with AlMe$_3$, BEt$_3$ or ZnEt$_2$ in the appropriate ratio. Complex **12b** has previously been reported (synthesis from H[PyrIm$^{i\mathrm{Pr}}$] with ZnSO$_4$ and KOH in methanol),[37] but NMR data in C$_6$D$_6$ was not provided. The complexes PyrIm$^{i\mathrm{Pr}}$-Me (**10a**) and PyrIm$^{i\mathrm{Pr}}$-Et (**10b**) formed slowly in the 1:1 reactions of MeI or EtI with Li(THF)$_x$[PyrIm$^{i\mathrm{Pr}}$][38] at 80 °C in benzene. However, they were more conveniently prepared by condensation of isopropylamine with the appropriate *N*-alkyl-2-pyrrolylaldehyde under Dean−Stark conditions with ZnCl$_2$ in benzene; **10a** and **10b** were isolated as colorless oils and characterized by NMR spectroscopy and HRMS.

All of the byproduct complexes discussed above are stable in solution with the exception of **12a**, which undergoes ligand redistribution to form an approximate 1: 1.4: 1.4 mixture of **12a**, **12b** and ZnEt$_2$ in benzene. Exchange of the PyrIm$^{i\mathrm{Pr}}$ ligands in **12a** and **12b**, and exchange of the ethyl groups in **12a** and ZnEt$_2$ was confirmed by 2D EXSY NMR spectroscopy at room temperature (Figure 6) and variable temperature ^{1}H and ^{13}C spectroscopy (Zn*Et* signals for **12a** and ZnEt$_2$ only become inequivalent below *ca.* −30 °C). However, slow evaporation from pentane provided crystals of pure **12a**, which were analyzed by single-crystal and powder (for the bulk sample) X-ray diffraction as well as combustion elemental analysis.

In the solid state, **12a** is dinuclear with two 3-coordinate [(PyrIm$^{i\mathrm{Pr}}$)ZnEt] units interacting through contacts between zinc and C(2) of the pyrrolyl ring (Figure 7). This same unusual bonding motif was recently reported for [(PyrIm$^{i\mathrm{Pr}}$)-Zn(CMe$_3$)],[39] although in **12a** the Zn−C(2) contact is shorter [2.664(3) vs 2.715(3) Å] and Zn is slightly more distorted toward pyramidal geometry [cent−Zn−C$_{\mathrm{alkyl}}$ = 157.3° vs 160.2°; cent = centroid of N(1) and N(2)], presumably due to reduced steric hindrance in **12a**. However, the Zn−C$_{\mathrm{alkyl}}$, Zn−N$_{\mathrm{pyrrolyl}}$ and Zn−N$_{\mathrm{imine}}$ distances of 1.967(3), 1.989(2) and 2.106(2) Å in **12a**, respectively, are very similar to those in the *tert*-butyl analogue. Structurally related and thermally stable [LZnR] complexes (*R* = Et or ^{t}Bu) were also reported using the 2,2′-(1′-pyrrolinyl)-pyrrole ligand, but in this case the crystal structure of the *tert*-butyl complex revealed dimer formation via Zn···N$_{\mathrm{pyrrolyl}}$ contacts, rather than Zn···C contacts.[40]

Complexes **9a** and **9b** are presumably tetrahedral and trigonal bipyramidal, respectively, and all methyl groups [^{1}H

(30) There was also no evidence for Cu[AlMe$_4$] formation. AlC*H*$_3$ ^{1}H NMR chemical shifts in the range 0.31 to −0.30 ppm have been reported for [Cp*$_2$La(AlMe$_4$)], [(ArO)$_2$Ln(AlMe$_4$)] (Ln = Lu, Y), [Ln(AlMe$_4$)$_3$] (Ln = Y, La, Lu), and [{Li(PNP)Li(AlMe$_4$)}$_2$], and AlC*H*$_3$ ^{1}H NMR chemical shifts of −0.18 to −0.36 ppm have been reported for the more separated ion pairs [ZnMe(14-N-4)][AlMe$_4$], [M(thf)$_6$][AlMe$_4$]$_2$ (M = Mg or Ca) and [{Ca(μ-OCH=CH$_2$)-(thf)$_4$}$_2$][AlMe$_4$]$_2$: (a) Dietrich, H. M.; Tornroos, K. W.; Herdtweck, E.; Anwander, R. *Organometallics* **2009**, *28*, 6739. (b) Fischbach, A.; Herdtweck, E.; Anwander, R.; Eickerling, G.; Scherer, W. *Organometallics* **2003**, *22*, 499. (c) Zimmermann, M.; Froystein, N. A.; Fischbach, A.; Sirsch, P.; Dietrich, H. M.; Tornroos, K. W.; Herdtweck, E.; Anwander, R. *Chem.—Eur. J.* **2007**, *13*, 8784. (d) Fryzuk, M. D.; Giesbrecht, G. R.; Rettig, S. J. *Organometallics* **1997**, *16*, 725. (e) Fabicon, R. M.; Richey, H. G., Jr. *Organometallics* **2001**, *20*, 4018. (f) Michel, O.; Meermann, C.; Törnroos, K. W.; Anwander, R. *Organometallics* **2009**, *28*, 4783.

(31) Whitesides, G. M.; SanFilippo, J. J.; Casey, C. P.; Panek, E. J. *J. Am. Chem. Soc.* **1967**, *89*, 5302.

(32) Goj, L. A.; Blue, E. D.; Delp, S. A.; Gunnoe, T. B.; Cundari, T. R.; Petersen, J. L. *Organometallics* **2006**, *25*, 4097.

(33) Miyamoto, R.; Santo, R.; Matsushita, T.; Nishioka, T.; Ichimura, A.; Teki, Y.; Kinoshita, I. *Dalton Trans.* **2005**, 3179.

(34) Kinoshita, I.; Wright, L. J.; Kubo, S.; Kimura, K.; Sakata, A.; Yano, T.; Miyamoto, R.; Nishioka, T.; Isobe, K. *Dalton Trans.* **2003**, 1993.

(35) Furuta, H.; Ishizuka, T.; Osuka, A.; Uwatoko, Y.; Ishikawa, Y. *Angew. Chem., Int. Ed.* **2001**, *40*, 2323. Chmielewski, P. J.; Latos-Grazynski, L.; Schmidt, I. *Inorg. Chem.* **2000**, *39*, 5475.

(36) Papasergio, R. I.; Raston, C. L.; White, A. H. *Dalton Trans.* **1987**, 3085.

(37) van Stein, G. C.; van Koten, G.; Passenier, H.; Steinebach, O.; Vrieze, K. *Inorg. Chim. Acta* **1984**, *89*, 79.

(38) Soluble Li(THF)$_x$[PyrIm$^{i\mathrm{Pr}}$] was prepared from benzene-insoluble Li[PyrIm$^{i\mathrm{Pr}}$] by addition of a small amount of THF.

(39) Lewinski, J.; Dranka, M.; Kraszewska, I.; Sliwinski, W.; Justyniak, I. *Chem. Commun.* **2005**, 4935.

(40) Lewinski, J.; Suwala, K.; Kaczorowski, T.; Galezowski, M.; Gryko, D. T.; Justyniak, I.; Lipkowski, J. *Chem. Commun.* **2009**, 215.

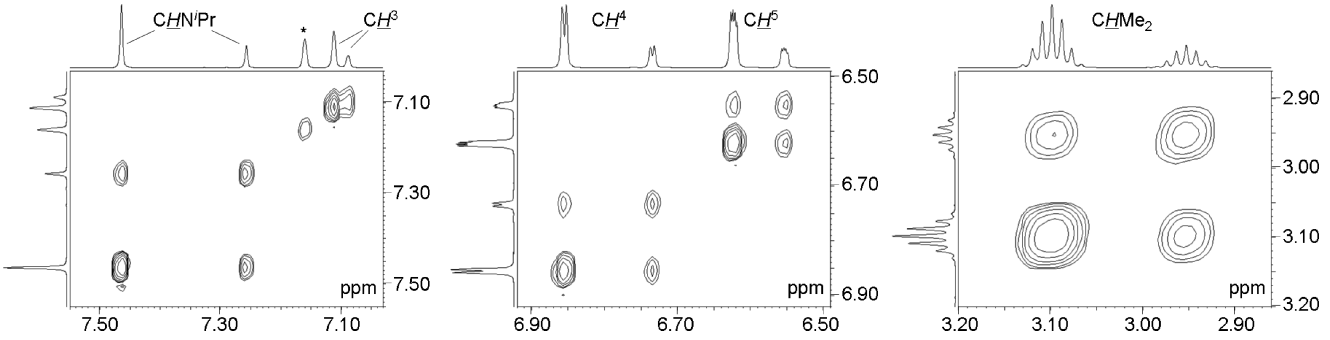

Figure 6. Selected regions of the 2D EXSY NMR spectrum after dissolution of solid [(PyrIm$^{i\mathrm{Pr}}$)ZnEt] (**12a**) in C_6D_6; in solution, **12a** exists in equilibrium with [Zn(PyrIm$^{i\mathrm{Pr}}$)$_2$] (**12b**) and $ZnEt_2$. For each PyrIm$^{i\mathrm{Pr}}$ ligand proton, the more intense peak corresponds to **12b**, and the less intense peak to **12a**.

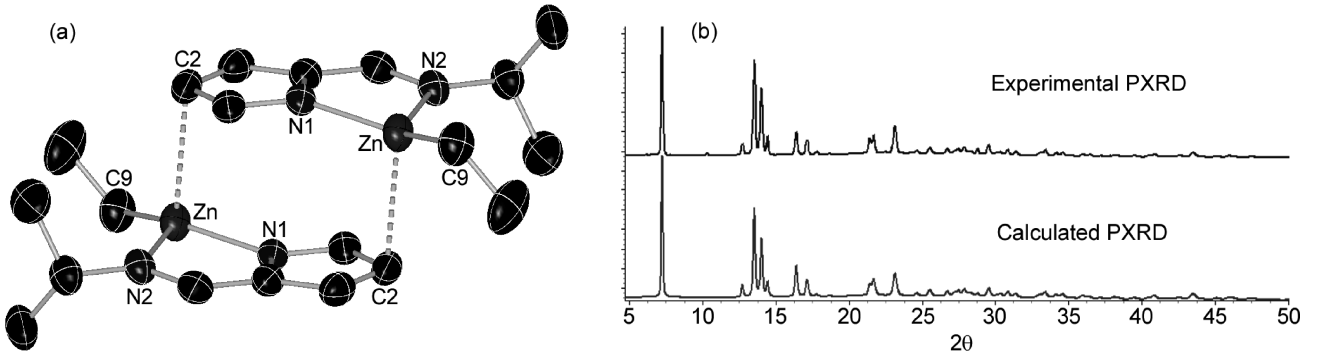

Figure 7. (a) Solid-state structure of **12a** with thermal ellipsoids at the 50% probability level. All hydrogen atoms are omitted for clarity. Selected bond lengths (Å) and angles (deg): Zn−N(1) = 1.989(2), Zn−N(2) = 2.106(2), Zn−C(9) = 1.967(3), Zn···C(2) = 2.664(3), N(1)−Zn−N(2) 82.62(7), N(1)−Zn−C(9) 142.09(10), N(2)−Zn−C(9) 127.07(12). (b) Experimental and calculated PXRD data.

NMR δ −0.32 ppm (**9a** and **9b**); ^{13}C NMR δ −8.8 ppm (**9a**); and −7.3 ppm (**9b**)] and PyrIm$^{i\mathrm{Pr}}$ ligands are equivalent by ^{1}H and ^{13}C NMR spectroscopy. Single crystals of **9b** suitable for X-ray crystallography were grown from hexanes at 20 °C and revealed a distorted trigonal bipyramidal geometry with all three anionic donors coordinated in equatorial positions (Figure 8; the unit cell contains two independent but isostructural molecules). By contrast, in the more sterically hindered [(L$^{\mathrm{DIPP}}$)$_2$AlCl] (L$^{\mathrm{DIPP}}$ = *N*-2,6-diisopropylphenyl-2-pyrrolylaldiminate) complex, the anionic pyrrolyl groups occupy apical sites of the trigonal bipyramid.[41] Presumably because of different arrangements of the ligands, the Al−N_{pyrrolyl} distances in **9b** [1.913(2)−1.922(2) Å] are shorter than the corresponding distances in [(L$^{\mathrm{DIPP}}$)$_2$AlCl] [1.962(1) Å], whereas the Al−N_{imine} bonds [2.081(2)−2.088(2) Å] are longer than those in [(L$^{\mathrm{DIPP}}$)$_2$AlCl] [1.993(1) Å], despite reduced steric hindrance at the imine donor of the PyrIm$^{i\mathrm{Pr}}$ ligand. These data are indicative of decreased delocalization of negative charge onto the imine groups in **9b**. The Al(1)−C(10) bond lengths of 1.973(2) and 1.967(2) Å in **9b** fall within the usual range for an aluminum alkyl complex (cf. 1.936(7) and 1.950(7) Å in [(L$^{\mathrm{DIPP}}$)AlMe$_2$] and 1.969(2) Å in [{MeC(N^{i}Pr)$_2$}$_2$AlMe]).[42]

In contrast to complex **9b** in which both PyrIm$^{i\mathrm{Pr}}$ ligands are equivalent, three distinct PyrIm$^{i\mathrm{Pr}}$ ligand environments were observed in the ^{1}H and ^{13}C NMR spectra of **9c**. These data are consistent with *mer*- rather than *fac*-octahedral geometry (Figure 3). A trigonal bipyramidal structure in which one PyrIm$^{i\mathrm{Pr}}$ ligand is κ^1-coordinated in an equatorial position, and the anionic pyrrolyl donors of the two κ^2-coordinated ligands occupy axial and equatorial sites, is also consistent with the NMR data. However, such a structure is unlikely given that the three PyrIm$^{i\mathrm{Pr}}$ ligands in **9c** show no signs of exchange, even at 80 °C.

Complexes **11a** and **12b** must adopt tetrahedral geometries,[43] and for **11a**, although both ethyl groups are equivalent, two doublets of quartets were observed in the ^{1}H NMR spectrum at 0.87 and 0.69 ppm due to diastereotopic BCH_2 protons. However, while **11a** was readily prepared by reaction of H[PyrIm$^{i\mathrm{Pr}}$] with BEt_3, reaction of BEt_3 with more than 1 equiv. of H[PyrIm$^{i\mathrm{Pr}}$] did not result in the formation of [(PyrIm$^{i\mathrm{Pr}}$)$_2$BEt] or [B(PyrIm$^{i\mathrm{Pr}}$)$_3$] at temperatures up to 110 °C. This observation is in keeping with the inability of **11a** to react with either [Cu(PyrIm$^{i\mathrm{Pr}}$)$_2$] (**6a**) or [Cu$_2$(PyrIm$^{i\mathrm{Pr}}$)$_2$] (**8**) at temperatures up to 100 °C. By contrast, H[PyrIm$^{i\mathrm{Pr}}$] reacted readily with $AlMe_3$ and $ZnEt_2$ to form **9a**−**9c**, **12a**, and **12b**. The low reactivity of **11a** may be attributed to the typical inability of boron to adopt a coordination number

(41) Hao, H. J.; Bhandari, S.; Ding, Y. Q.; Roesky, H. W.; Magull, J.; Schmidt, H. G.; Noltemeyer, M.; Cui, C. M. *Eur. J. Inorg. Chem.* **2002**, 1060.

(42) Liang, L. C.; Yang, C. W.; Chiang, M. Y.; Hung, C. H.; Lee, P. Y. *J. Organomet. Chem.* **2003**, *679*, 135. Rowley, C. N.; DiLabio, G. A.; Barry, S. T. *Inorg. Chem.* **2005**, *44*, 1983.

(43) Zinc bis(pyrrolylaldiminate) complexes, [ZnL$_2$] (L = *N*-2,6-diisopropylphenyl-2-pyrrolylaldiminate and the 5-*tert*-butyl-substituted analogue), have been reported.[41]

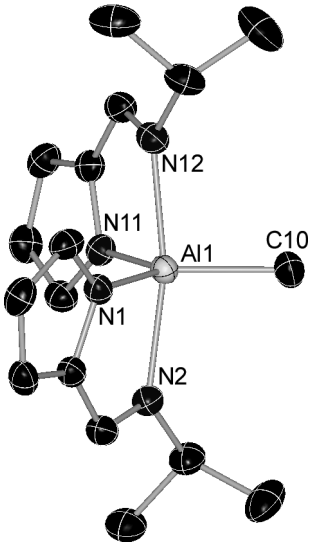

Figure 8. Solid-state structure of **9b** with thermal ellipsoids at the 50% probability level. Only one of the two independent molecules in the unit cell is shown. All hydrogen atoms are omitted for clarity. Selected bond lengths (Å) and angles (deg): Al(1)−N(1) = 1.922(2), Al(1)−N(11) = 1.918(2), Al(1)−N(2) = 2.088(2), Al(1)−N(12) = 2.084(2), Al(1)−C(10) = 1.973(2), N(1)−Al(1)−N(2) = 80.66(7), N(11)−Al(1)−N(12) = 80.51(7), N(2)−Al(1)−N(12) = 167.81(7), N(1)−Al(1)−N(11) = 115.87(7), N(1)−Al(1)−C(10) = 121.16(9), N(11)−Al(1)−C(10)=122.97(9). Al(2)−N(21)=1.916(2), Al(2)−N(31) = 1.913(2), Al(2)−N(22) = 2.086(2), Al(2)−N(32) = 2.081(2), Al(2)−C(20) = 1.967(2), N(21)−Al(2)−N(22) = 80.83(7), N(31)−Al(2)−N(32) = 80.98(8), N(22)−Al(2)−N(32)=169.83(7), N(21)−Al(2)−N(31)=116.89(8), N(21)−Al(2)−C(20) = 120.39(9), N(31)−Al(2)−C(20) = 122.70(9). In molecule 2 in the unit cell, Al(2), N(21), N(22), N(31), N(32), and C(20) are equivalent to Al(1), N(1), N(2), N(11), N(12), and C(10) in molecule 1.

Table 1. Volatility and Thermal Stability Data for Byproducts 8, 9a−9c, 10a, 10b, 11a, and 12a, 12b

compd	volatility/thermal stability data at 1×10^{-2} Torr
$[Cu_2(PyrIm^{iPr})_2]$ (**8**)	decomposes at 180 °C without sublimation
$[(PyrIm^{iPr})AlMe_2]$ (**9a**)	melts and distills at 60 °C
$[(PyrIm^{iPr})_2AlMe]$ (**9b**)	sublimes at 90 °C
$[Al(PyrIm^{iPr})_3]$ (**9c**)	sublimes at 110 °C
$PyrIm^{iPr}$−Me (**10a**)	distills at ∼45 °C
$PyrIm^{iPr}$−Et (**10b**)	distills at ∼45 °C
$[(PyrIm^{iPr})BEt_2]$ (**11a**)	distills at < 20 °C
$[(PyrIm^{iPr})ZnEt]$ (**12a**)	attempted sublimation at 70 °C yielded only **12b**; ligand redistribution to $ZnEt_2$ and **12b** therefore occurs in the solid state at ≤70 °C.
$[Zn(PyrIm^{iPr})_2]$ (**12b**)	sublimes slowly at 70 °C, rapidly at 85 °C

greater than four, combined with tight chelation of the $PyrIm^{iPr}$ ligand in **11a**.

Reaction Byproduct Thermal Stability. The thermal stability and volatility of complexes $[Cu_2(PyrIm^{iPr})_2]$ (**8**), $[(PyrIm^{iPr})AlMe_2]$ (**9a**), $[(PyrIm^{iPr})_2AlMe]$ (**9b**), $[Al(PyrIm^{iPr})_3]$ (**9c**), $PyrIm^{iPr}$-Me (**10a**), $PyrIm^{iPr}$-Et (**10b**), $[(PyrIm^{iPr})BEt_2]$ (**11a**), $[(PyrIm^{iPr})ZnEt]$ (**12a**) and $[Zn(PyrIm^{iPr})_2]$ (**12b**) were investigated by distillation or sublimation in vacuo. The results of these investigations are summarized in Table 1, and are of importance to ALD performance because of the requirement for reaction byproducts to be removed in vacuo without thermal decomposition to nonvolatile byproducts.

Only complexes **8** and **12a** fail to sublime or distill in vacuo; complex **8** is insufficiently volatile and decomposes at high temperature, while **12a** undergoes facile ligand redistribution at 70 °C or below. For the remaining complexes, an important observation is that products containing a single $PyrIm^{iPr}$ ligand (**9a**, **10a**, **10b** and **11a**) are substantially more volatile than those bearing multiple $PyrIm^{iPr}$ ligands, so are more desirable as byproducts of ALD. The inability of $[(PyrIm^{iPr})BEt_2]$ (**11a**) to react further with **6a** or **8** to form bis- or tris-ligand complexes may therefore be a beneficial feature for ALD of pure metal films. However, this advantage is offset by the greatly reduced reactivity of BEt_3 (relative to $AlMe_3$ and $ZnEt_2$), which has rendered this coreagent ineffective for copper metal ALD or pulsed-CVD.[3] That said, the bis-ligand complexes **9b** and **12b** (and to a lesser extent tris-ligand complex **9c**) are still sufficiently volatile to allow their removal during an ALD process operating in the 110−130 °C regime.

Summary and Conclusions

To provide a starting point for the analysis and understanding of surface reactivity responsible for metal ALD/pulsed-CVD, the solution reactions of bis(*N*-isopropylpyrrolylaldiminate)copper(II) ($[Cu(PyrIm^{iPr})_2]$; **6a**) with $AlMe_3$, BEt_3, and $ZnEt_2$ have been studied. In each case, reduction occurs in two stages via a stable dinuclear copper(I) pyrrolylaldiminate complex (**8**), with each stage initiated by copper alkyl complex formation. Reduction from "$(PyrIm^{iPr})CuR$" (R = Me or Et) occurs with release of R_2 or $PyrIm^{iPr}$-R, consistent with bimolecular C−C or C−N bond-forming reductive elimination. At room temperature or below, copper deposition from "CuMe" occurs exclusively via reductive elimination of ethane, whereas decomposition of "CuEt" yields ethylene, ethane, and hydrogen, indicative of both β-hydride elimination and reductive elimination. In the presence of an excess of the more reactive reagents $AlMe_3$ and $ZnEt_2$, it was not possible to rule out initial double alkylation to form a highly unstable copper(II) dialkyl species. However, if "CuR_2" does form, it must decompose to "CuR" rather than to copper metal, since under these conditions (an excess of $AlMe_3$ or $ZnEt_2$), copper metal formation is not observed at temperatures where "CuR" is stable. The intermediates and byproducts $[Cu_2(PyrIm^{iPr})_2]$ (**8**), $[(PyrIm^{iPr})AlMe_2]$ (**9a**), $[(PyrIm^{iPr})_2AlMe]$ (**9b**), $[Al(PyrIm^{iPr})_3]$ (**9c**), $PyrIm^{iPr}$-Me (**10a**), $PyrIm^{iPr}$-Et (**10b**), $[(PyrIm^{iPr})BEt_2]$ (**11a**), $[(PyrIm^{iPr})ZnEt]$ (**12a**), and $[Zn(PyrIm^{iPr})_2]$ (**12b**) were prepared independently in pure form, and characterized by NMR spectroscopy and in some cases X-ray crystallography. All byproducts are thermally stable, with the exception of **12a**, which undergoes ligand redistribution to form **12b** and $ZnEt_2$ at elevated temperatures and in solution. Of the stable organometallic complexes, monoligated $[(PyrIm^{iPr})AlMe_2]$ (**9a**) and $[(PyrIm^{iPr})BEt_2]$ (**11a**) are particularly volatile, so are more desirable as byproducts in ALD or pulsed-CVD.

Experimental Section

An argon-filled MBraun UNIlab glovebox was employed for the manipulation and storage of all oxygen and moisture sensitive compounds, and air-sensitive preparative reactions

were performed on a double manifold high vacuum line using standard techniques.[44] Residual oxygen and moisture was removed from the argon stream by passage through an Oxisorb-W scrubber from Matheson Gas Products. A Fisher Scientific Ultrasonic FS-30 bath was used to sonicate reaction mixtures where indicated, and a Fischer Scientific model 228 Centrific Centrifuge in combination with airtight Kimble-Kontes 15 mL conical centrifuge tubes was used when required. Vacuum was measured using a Varian model 531 Thermocouple Gauge Tube with a Model 801 Controller. Combustion elemental analyses were performed on a Thermo EA1112 CHNS/O analyzer. Single-crystal X-ray crystallographic analyses were performed on crystals coated in Paratone oil and mounted on a SMART APEX II diffractometer with a 3 kW sealed tube Mo generator or a three circle Bruker D8 diffractometer with a Rigaku Cu rotating anode generator and SMART6000 CCD detector. Powder X-ray Diffraction (PXRD) experiments were performed on a Bruker D8 Advance Powder diffractometer with Cu Kα radiation ($\lambda = 0.154$ nm) operated at 40 kV and 40 mA. The powder pattern for **12a** was calculated from the low-temperature single-crystal data and then refined using Topas 4.2 (Bruker software).[45]

Anhydrous diethyl ether was purchased from Aldrich. Hexanes, toluene, and THF were initially dried and distilled at atmospheric pressure from CaH_2, sodium and sodium benzophenone ketyl, respectively. Unless otherwise noted, all anhydrous solvents were stored over an appropriate drying agent prior to use (OEt_2, THF, d_8-THF, toluene, d_8-toluene, C_6D_6 = Na/Ph_2CO; pentane, hexanes = Na/Ph_2CO/tetraglyme). 2-Pyrrolylaldehyde, *N*-methyl-2-pyrrolylaldehyde, isopropylamine, MeI, EtI, ^{n}BuLi (1.6 M in hexane), $ZnCl_2$, and CuCl were purchased from Aldrich or Strem Chemicals. *N*-Ethyl-2-pyrrolylaldehyde,[46] *N*-isopropyl-2-pyrrolylaldimine (H[PyrIm^{iPr}]),[37] mesityl copper(I),[47] **6a**[48] and **7**[49] were prepared as described in the literature. $AlMe_3$ (98%), $ZnEt_2$ (min. 95%), and BEt_3 (98%) were purchased in metal cylinders from Strem chemicals and stored within an argon-filled glovebox. ***Note:*** *$AlMe_3$, $ZnEt_2$, and BEt_3 are strongly pyrophoric liquids and so must be handled only under strict air-free conditions.*

[{Cu(PyrIm^{iPr})}$_2$] (8). Method A: A solution of H[PyrIm^{iPr}] (0.136 g, 1.0 mmol) in toluene (10 mL) was added to the toluene solution (10 mL) of mesityl copper(I) (0.181 g, 0.33 mmol). The solution changed color to bright yellow and stirring was continued for 2 h. The solvent was removed in vacuo, and the residue was redissolved in toluene (5 mL). The mixture was then centrifuged to remove any insoluble material, and the centrifugate was layered with hexanes at −30 °C to yield a pale yellow solid which was dried in vacuo (0.170 g, 0.427 mmol, 85%). Method B: Li[PyrIm^{iPr}] (0.100 g, 0.704 mmol) and CuCl (0.767 g, 0.775 mmol) in THF (10 mL) were stirred overnight at room temperature. The solvent was completely removed in vacuo, and the residue was redissolved in toluene (5 mL). The mixture was then centrifuged to discard insoluble LiCl and the centrifugate was layered with hexanes at −30 °C to yield X-ray quality pale yellow crystals of **8**·0.5toluene which were dried in vacuo to yield toluene-free **8** (0.115 g, 0.289 mmol, 82%). ^{1}H NMR (C_6D_6, 600 MHz): δ 7.59 (broad s, 1H, C*H*N^{i}Pr$_2$), 7.45 (broad s, 1H, C*H*^{5}), 6.91 (dd, 1H, $^3J_{H,H}$ 3.5, 1.0 Hz, C*H*^{3}), 6.66 (broad s, 1H, C*H*^{4}), 2.84 (sept, 1H, $^3J_{H,H}$ 6 Hz, C*H*Me$_2$), 0.97 (d, 6H, $^3J_{H,H}$ 6 Hz, CH*Me*$_2$). ^{13}C{^{1}H} NMR (C_6D_6, 151 MHz): δ 159.22 (*C*HN^{i}Pr$_2$), 138.18 (*C*H^5), 135.06 (*C*^{2}), 125.20 (*C*H^3), 112.55 (*C*H^4), 62.35 (*C*HMe$_2$), 25.66 (CH*Me*$_2$). Anal. Calcd for $C_{16}H_{22}N_4Cu_2$: C 48.35, H 5.58, N 14.10. Found: C 48.82, H 5.66, N 13.80%.

[(PyrIm^{iPr})AlMe$_2$] (9a). A solution of $AlMe_3$ in 2 mL toluene (0.053 g, 0.735 mmol) was added to H[PyrIm^{iPr}] (0.100 g, 0.735 mmol) in toluene (3 mL) at −30 °C. The solution was warmed to room temperature to give a bright yellow solution and stirred for 1 h. It was then evaporated to dryness in vacuo, redissolved in pentane, and cooled to −30 °C to yield **9a** as a pale yellow crystalline solid (0.115 g, 0.598 mmol, 81%). ^{1}H NMR (C_6D_6, 600 MHz): δ 7.08 (broad s, 1H, C*H*^{5}), 7.04 (s, 1H, C*H*N^{i}Pr$_2$), 6.69 (d, 1H, $^3J_{H,H}$ 3.5 Hz, C*H*^{3}), 6.42 (dd, 1H, $^3J_{H,H}$ 3.5, 1.9 Hz, C*H*^{4}), 2.96 (sept, 1H, $^3J_{H,H}$ 7 Hz, C*H*Me$_2$), 0.09 (d, 6H, $^3J_{H,H}$ 7 Hz, CH*Me*$_2$), −0.32 (s, 6H, Al*Me*$_2$). ^{13}C{^{1}H} NMR (C_6D_6, 151 MHz): δ 158.19 (*C*HN^{i}Pr$_2$), 135.35 (*C*^{2}), 134.82 (*C*H^5), 118.65 (*C*H^3), 114.78 (*C*H^4), 55.63 (*C*HMe$_2$), 23.92 (CH*Me*$_2$), −8.8 (broad s, Al*Me*$_2$). Anal. Calcd for $C_{10}H_{17}N_2Al$: C 62.48, H 8.91, N 14.57. Found: C 62.26, H 9.02, N 14.44%.

[(PyrIm^{iPr})$_2$AlMe] (9b). A solution of H[PyrIm^{iPr}] (0.340 g, 2.500 mmol) in hexanes (4 mL) was added dropwise to $AlMe_3$ in 5 mL hexanes (0.100 g, 1.390 mmol) at −78 °C. The solution was warmed to room temperature over 2 h to give a colorless solution, which was evaporated to dryness and dried in vacuo overnight. The crude product was then redissolved in hot hexanes and cooled to −30 °C to obtain **9b** as a colorless crystalline solid (0.290 g, 0.928 mmol, 81%). ^{1}H NMR (C_6D_6, 600 MHz): δ 7.67 (s, 1H, C*H*N^{i}Pr$_2$), 7.12 (broad s, 1H, C*H*^{5}), 6.73 (m, 1H, C*H*^{3}), 6.52 (m, 1H, C*H*^{4}), 3.79 (sept, 1H, $^3J_{H,H}$ 7 Hz, C*H*Me$_2$), 1.01 (d, 6H, $^3J_{H,H}$ 7 Hz, CH*Me*$_2$), −0.32 (s, 3H, Al*Me*). ^{13}C{^{1}H} NMR (C_6D_6, 151 MHz): δ 155.39 (*C*HN^{i}Pr$_2$), 136.93 (*C*^{2}), 133.59 (*C*H^5), 116.49 (*C*H^3), 113.12 (*C*H^4), 50.16 (*C*HMe$_2$), 23.5 (CH*Me*$_2$), −7.3 (broad s, Al*Me*). Anal. Calcd for $C_{17}H_{25}N_4Al$: C 65.36, H 8.07, N 17.93. Found: C 65.06, H 8.24, N 18.24%.

[(PyrIm^{iPr})$_3$Al] (9c). A solution of $AlMe_3$ in 2 mL toluene (0.018 g, 0.245 mmol) was added to H[PyrIm^{iPr}] (0.100 g, 0.735 mmol) in toluene (3 mL) at −30 °C. The solution was warmed to room temperature to give a pale yellow solution and stirred for 1 h. It was then dried in vacuo overnight, redissolved in hot hexanes, and cooled to −30 °C to obtain the product as a colorless crystalline solid (0.093 g, 0.212 mmol, 87%). ^{1}H NMR (C_6D_6, 600 MHz): δ 7.77, 7.76, 7.74 (s, 3 × 1H, C*H*N^{i}Pr$_2$), 7.13, 7.04, 6.48 (dd, 3 × 1H, $^3J_{H,H}$ 1.8 Hz, $^4J_{H,H}$ 1 Hz, C*H*^{5}), 6.86, 6.76, 6.73 (dd, 3 × 1H, $^3J_{H,H}$ 3.5 Hz, $^4J_{H,H}$ 1 Hz, C*H*^{3}), 6.56, 6.46, 6.38 (dd, 3 × 1H, $^3J_{H,H}$ 3.5, 1.8 Hz, C*H*^{4}), 3.66, 3.34, 3.08 (sept, 3 × 1H, $^3J_{H,H}$ 7 Hz, C*H*Me$_2$), 1.00, 0.91, 0.84, 0.69, 0.68, 0.54 (d, 3 × 6H, $^3J_{H,H}$ 7 Hz, CH*Me*$_2$). ^{13}C{^{1}H} NMR (C_6D_6, 151 MHz): δ 156.27, 155.55, 154.43 (*C*HN^{i}Pr$_2$), 135.56, 135.23, 135.04 (*C*^{2}), 134.37, 132.58, 132.30 (*C*H^5), 116.34, 115.99, 115.95 (*C*H^3), 113.31, 112.58, 112.30 (*C*H^4), 50.89, 49.94, 49.57 (*C*HMe$_2$), 25.00, 24.14, 24.01, 22.52, 21.91 (CH*Me*$_2$). Anal. Calcd for $C_{24}H_{33}N_6Al$: C 66.64, H 7.69, N 19.43. Found: C 66.53, H 7.83, N 19.54%.

PyrIm^{iPr}-Me (10a). To 1-Methyl-1*H*-pyrrole-2carboxaldehyde (0.200 g, 1.833 mmol) and isopropylamine (0.19 mL,

(44) Burger, B. J.; Bercaw, J. E. Vacuum Line Techniques for Handling Air-Sensitive Organometallic Compounds. In *Experimental Organometallic Chemistry−A Practicum in Synthesis and Characterization*; American Chemical Society: Washington D.C., 1987; Vol. *357*, p 79.
(45) The refined cell had a greater volume than the original because powder diffraction was performed at room temperature, whereas the single-crystal experiment was performed at low temperature.
(46) Soares, M. I. L.; Lopes, S. M. M.; Cruz, P. F.; Brito, R. M. M.; Pinho e Melo, T. M. V. D. *Tetrahedron* **2008**, *64*, 9745.
(47) Tsuda, T.; Yazawa, T.; Watanabe, K.; Fujii, T.; Saegusa, T. *J. Org. Chem.* **1981**, *46*, 192.
(48) Holm, R. H.; Chakravorty, A.; Theriot, L. J. *Inorg. Chem.* **1966**, *5*, 625. Yokoi, H.; Addison, A. W. *Inorg. Chem.* **1977**, *16*, 1341. Grushin, V. V.; Marshall, W. J. *Adv. Synth. Catal.* **2004**, *346*, 1457.
(49) Sacconi, L.; Ciampolini, M. *J. Chem. Soc.* **1964**, 267. Orioli, P. L.; Sacconi, L. *J. Am. Chem. Soc.* **1966**, *88*, 277.

2.199 mmol) in benzene (10 mL) in a Dean−Stark apparatus, a catalytic amount of $ZnCl_2$ was added. The mixture was refluxed at 85 °C for 2 h to remove the benzene-water azeotrope. It was then filtered and the solvent was removed to give yellow oil, which was distilled at 45 °C (10 mTorr) to collect the product as a colorless oil. Yield: 0.259 g, 94%. ^{1}H NMR (C_6D_6, 500 MHz): δ 7.99 (s, 1H, C*H*N^{i}Pr$_2$), 6.44 (m, 1H, C*H*^{3}), 6.31 (broad s, 1H, C*H*^{5}), 6.15 (app t, 1H, $J_{H,H}$ 3 Hz, C*H*^{4}), 3.61 (s, 3H, NC*H*$_3$), 3.15 (sept, 1H, $^3J_{H,H}$ 7 Hz, C*H*Me$_2$), 1.21 (d, 6H, $^3J_{H,H}$ 7 Hz, CH*Me*$_2$). ^{13}C{^{1}H} NMR (C_6D_6, 125 MHz): δ 150.11 (*C*HN^{i}Pr$_2$), 130.33 (*C*^{2}), 127.65 (*C*H^5), 116.78 (*C*H^3), 108.22 (*C*H^4), 62.52 (*C*HMe$_2$), 36.56 (s, N*C*H$_3$), 24.94 (CH*Me*$_2$). HRMS for $C_9H_{14}N_2$ (M^+): found 150.1163, calcd 150.1157.

PyrIm^{iPr}-Et (10b). Compound **10b** was prepared following the procedure for **10a**, but using 1-ethyl-1*H*-pyrrole-2-carboxaldehyde (0.200 g, 1.624 mmol) and isopropylamine (0.17 mL, 1.949 mmol). The product was obtained as colorless oil (0.250 g, 94%) after distillation at 45 °C (10 mTorr). ^{1}H NMR (C_6D_6, 500 MHz): δ 7.97 (s, 1H, C*H*N^{i}Pr$_2$), 6.44 (dd, 1H, $J_{H,H}$ 3.7, 1.8 Hz, C*H*^{3}), 6.42 (dd, $J_{H,H}$ 2.6, 1.8 Hz, 1H, C*H*^{5}), 6.17 (dd, 1H, $J_{H,H}$ 3.7, 2.6 Hz, C*H*^{4}), 4.19 (q, 2H, $^3J_{H,H}$ 7 Hz, NC*H*$_2$), 3.14 (sept, 1H, $^3J_{H,H}$ 7 Hz, C*H*Me$_2$), 1.19 (d, 6H, $^3J_{H,H}$ 7 Hz, CH*Me*$_2$), 1.12 (t, 3H, $^3J_{H,H}$ 7 Hz, NCH$_2$C*H*$_3$). ^{13}C{^{1}H} NMR (C_6D_6, 125 MHz): δ 150.10 (*C*HN^{i}Pr$_2$), 129.76 (*C*^{2}), 126.51 (*C*H^5), 117.76 (*C*H^3), 108.67 (*C*H^4), 62.76 (*C*HMe$_2$), 44.05 (s, N*C*H$_2$), 25.18 (CH*Me*$_2$), 17.19 (NCH$_2$*C*H$_3$). HRMS for $C_{10}H_{16}N_2$ (M^+): found 164.1309, calcd 164.1313.

[(PyrIm^{iPr})BEt$_2$] (11a). A solution of BEt_3 in 2 mL hexanes (0.080 g, 0.809 mmol) was added to H[PyrIm^{iPr}] (0.100 g, 0.735 mmol) in toluene (3 mL) at −30 °C, and the solution was warmed to room temperature and stirred for 18 h. The resulting yellow solution was evaporated to dryness in vacuo at 0 °C to obtain the product as a pale yellow oil (0.128 g, 0.627 mmol, 85%). ^{1}H NMR (C_6D_6, 600 MHz): δ 7.13 (s, 1H, C*H*N^{i}Pr$_2$), 7.12 (broad s, 1H, C*H*^{5}), 6.65 (d, 1H, $^3J_{H,H}$ 3.5 Hz, C*H*^{3}), 6.53 (dd, 1H, $^3J_{H,H}$ 3.4, 1.7 Hz, C*H*^{4}), 3.42 (sept, 1H, $^3J_{H,H}$ 7 Hz, C*H*Me$_2$), 0.82 (d, 6H, $^3J_{H,H}$ 7 Hz, CH*Me*$_2$), 0.73 (app t, $^3J_{H,H}$ 7 Hz, 6H, BCH$_2$C*H*$_3$), 0.87, 0.68 (dq, $^2J_{H,H}$ 14 Hz, $^3J_{H,H}$ 7 Hz, 4H, BC*H*$_2$CH$_3$). ^{13}C{^{1}H} NMR (C_6D_6, 151 MHz): δ 149.90 (*C*HN^{i}Pr$_2$), 135.05 (*C*^{2}), 128.39 (*C*H^5), 115.05 (*C*H^4), 110.80 (*C*H^3), 48.80 (*C*HMe$_2$), 23.54 (CH*Me*$_2$), 14.80 (B*C*H$_2$CH$_3$), 9.17 (BCH$_2$*C*H$_3$). HRMS for $C_{12}H_{21}N_2B$ (M^+): found 204.1797, calcd 204.1798.

[(PyrIm^{iPr})ZnEt] (12a). A solution of H[PyrIm^{iPr}] (0.200 g, 1.470 mmol) in pentane (2 mL) was added dropwise over 3−5 min to $ZnEt_2$ in 5 mL pentane (150 μL, 1.470 mmol) at −78 °C. The solution was warmed slowly over 1 h to room temperature to give a peach colored solution. It was then dried in vacuo at 0 °C, redissolved in pentane, and cooled to −30 °C to obtain the product as a colorless crystalline solid (0.240 g, 1.048 mmol, 78%). Upon dissolution, solid **12a** undergoes ligand redistribution to form a mixture of **12a**, **12b**, and $ZnEt_2$ (1:1.4:1.4 ratio at 20 °C). NMR data is given only for **12a** unless otherwise indicated. ^{1}H NMR (C_6D_6, 600 MHz): δ 7.26 (s, 1H, C*H*N^{i}Pr$_2$), 7.09 (broad s, 1H, C*H*^{5}), 6.73 (d, 1H, $^3J_{H,H}$ 3.5 Hz, C*H*^{3}), 6.55 (m, 1H, C*H*^{4}), 2.95 (sept, 1H, $^3J_{H,H}$ 7 Hz, C*H*Me$_2$), 1.22 (broad s, 6H, ZnCH$_2$C*H*$_3$ with fast ethyl group exchange between **12a** and $ZnEt_2$), 0.84 (d, 6H, $^3J_{H,H}$ 7 Hz, CH*Me*$_2$), 0.24 (broad s, 4H, ZnC*H*$_2$ with fast ethyl group exchange between **12a** and $ZnEt_2$). ^{13}C{^{1}H} NMR (C_6D_6, 151 MHz): δ 157.64 (*C*HN^{i}Pr$_2$), 137.07 (*C*^{2}), 135.32 (*C*H^5), 117.47 (*C*H^3), 113.21 (*C*H^4), 56.79 (*C*HMe$_2$), 24.32 (CH*Me*$_2$), 11.31 (ZnCH$_2$*C*H$_3$ with fast ethyl group exchange between **12a** and $ZnEt_2$). ^{1}H NMR (C_7D_8, 500 MHz, −70 °C): δ 1.78 (broad s, 6H, ZnCH$_2$C*H*$_3$), 0.72 (broad s, 4H, ZnC*H*$_2$). ^{13}C{^{1}H} NMR (C_7D_8, 125 MHz, −70 °C): δ 14.11 (ZnCH$_2$*C*H$_3$), 1.81 (Zn*C*H$_2$). Anal. Calcd for $C_{10}H_{16}N_2Zn$: C 52.30, H 7.02, N 12.20. Found: C 52.24, H 7.01, N 12.41%.

[(PyrIm^{iPr})$_2$Zn] (12a). A solution of $ZnEt_2$ in 2 mL hexanes (0.045 g, 0.367 mmol) was added to H[PyrIm^{iPr}] (0.100 g, 0.735 mmol) in hexanes (3 mL) at −30 °C. The solution was warmed to room temperature to give a colorless solution and stirred for 1 h. It was then evaporated to dryness in vacuo, redissolved in pentane, and cooled to −30 °C to obtain the product as a colorless solid (0.215 g, 0.640 mmol, 87%). ^{1}H NMR (C_6D_6, 600 MHz): δ 7.48 (s, 1H, C*H*N^{i}Pr$_2$), 7.09 (broad s, 1H, C*H*^{5}), 6.84 (d, 1H, $^3J_{H,H}$ 3.5 Hz, C*H*^{3}), 6.60 (dd, 1H, $^3J_{H,H}$ 3.5, 1.8 Hz, C*H*^{4}), 3.12 (sept, 1H, $^3J_{H,H}$ 6.5 Hz, C*H*Me$_2$), 0.85 (d, 6H, $^3J_{H,H}$ 6.4 Hz, CH*Me*$_2$). ^{13}C{^{1}H} NMR (C_6D_6, 151 MHz): δ 157.64 (*C*HN^{i}Pr$_2$), 136.60 (*C*^{2}), 135.25 (*C*H^5), 117.50 (*C*H^3), 113.41 (*C*H^4), 57.27 (*C*HMe$_2$), 24.52 (CH*Me*$_2$). Anal. Calcd for $C_{16}H_{22}N_4Zn$: C 57.25, H 6.56, N 16.69. Found: C 56.93, H 6.65, N 16.47%.

Li[PyrIm^{iPr}]. A 1.6 M solution of ^{n}BuLi in hexane (5.06 mL, 8.088 mmol) was added to H[PyrIm^{iPr}] (1.000 g, 7.353 mmol) in hexanes (30 mL) at −78 °C. After stirring for 10 min the solution was warmed to room temperature to give a colorless solution with large amount of white precipitate. It was then filtered, washed with hexanes (×2) and dried in vacuo to obtain the product as a white solid (0.910 g, 6.408 mmol, 87%). ^{1}H NMR (d_8-THF, 600 MHz): δ 7.88 (s, 1H, C*H*N^{i}Pr$_2$), 6.82 (broad s, 1H, C*H*^{5}), 6.29 (m, 1H, C*H*^{3}), 5.93 (m, 1H, C*H*^{4}), 3.33 (sept, 1H, $^3J_{H,H}$ 7 Hz, C*H*Me$_2$), 1.16 (d, 6H, $^3J_{H,H}$ 7 Hz, CH*Me*$_2$). ^{13}C{^{1}H} NMR (d_8-THF, 151 MHz): δ 158.56 (*C*HN^{i}Pr$_2$), 139.38 (*C*^{2}), 134.59 (*C*H^5), 115.75 (*C*H^3), 109.29 (*C*H^4), 59.71 (*C*HMe$_2$), 25.81 (CH*Me*$_2$). Anal. Calcd for $C_8H_{11}N_2Li$: C 67.61, H 7.80, N 19.71. Found: C 67.03, H 7.87, N 18.87%.

Acknowledgment. D.J.H.E. is grateful for funding provided by Intel Corporation and the Emerging Materials Knowledge (EMK) program of Ontario Centres of Excellence (OCE), Canada. We also thank Victoria M. Jarvis of the McMaster Analytical X-ray Diffraction Facility for collection and refinement of PXRD data.

Supporting Information Available: NMR spectra and tables of crystallographic data (PDF). This material is available free of charge via the Internet at http://pubs.acs.org.